

On the Robustness of Domain Constraints

Ryan Sheatsley

The Pennsylvania State University
State College, Pennsylvania, USA
sheatsley@psu.edu

Blaine Hoak

The Pennsylvania State University
State College, Pennsylvania, USA
bhoak@psu.edu

Eric Pauley

The Pennsylvania State University
State College, Pennsylvania, USA
epauley@psu.edu

Yohan Beugin

The Pennsylvania State University
State College, Pennsylvania, USA
ybeugin@psu.edu

Michael J. Weisman

United States Army Combat
Capabilities Development Command
Army Research Laboratory
Adelphi, Maryland, USA
michael.j.weisman2.civ@army.mil

Patrick McDaniel

The Pennsylvania State University
State College, Pennsylvania, USA
mcdaniel@cse.psu.edu

ABSTRACT

Machine learning is vulnerable to *adversarial examples*—inputs designed to cause models to perform poorly. However, it is unclear if adversarial examples represent realistic inputs in the modeled domains. Diverse domains such as networks and phishing have *domain constraints*—complex relationships between features that an adversary must satisfy for an attack to be realized (in addition to any adversary-specific goals). In this paper, we explore how domain constraints limit adversarial capabilities and how adversaries can adapt their strategies to create realistic (constraint-compliant) examples. In this, we develop techniques to learn domain constraints from data, and show how the learned constraints can be integrated into the adversarial crafting process. We evaluate the efficacy of our approach in network intrusion and phishing datasets and find: (1) up to 82% of adversarial examples produced by state-of-the-art crafting algorithms violate domain constraints, (2) domain constraints are robust to adversarial examples; enforcing constraints yields an increase in model accuracy by up to 34%. We observe not only that adversaries must alter inputs to satisfy domain constraints, but that these constraints make the generation of valid adversarial examples far more challenging.

CCS CONCEPTS

• **Security and privacy** → **Formal methods and theory of security**; • **Computing methodologies** → **Machine learning**.

KEYWORDS

adversarial machine learning; constraint learning; constraint satisfaction; formal logic

ACM Reference Format:

Ryan Sheatsley, Blaine Hoak, Eric Pauley, Yohan Beugin, Michael J. Weisman, and Patrick McDaniel. 2021. On the Robustness of Domain Constraints.

Permission to make digital or hard copies of all or part of this work for personal or classroom use is granted without fee provided that copies are not made or distributed for profit or commercial advantage and that copies bear this notice and the full citation on the first page. Copyrights for components of this work owned by others than the author(s) must be honored. Abstracting with credit is permitted. To copy otherwise, or republish, to post on servers or to redistribute to lists, requires prior specific permission and/or a fee. Request permissions from permissions@acm.org.

CCS '21, November 15–19, 2021, Virtual Event, Republic of Korea

© 2021 Copyright held by the owner/author(s). Publication rights licensed to ACM.

ACM ISBN 978-1-4503-8454-4/21/11...\$15.00

<https://doi.org/10.1145/3460120.3484570>

In *Proceedings of the 2021 ACM SIGSAC Conference on Computer and Communications Security (CCS '21)*, November 15–19, 2021, Virtual Event, Republic of Korea. ACM, New York, NY, USA, 21 pages. <https://doi.org/10.1145/3460120.3484570>

1 INTRODUCTION

Machine learning has demonstrated exceptional problem-solving capabilities; it has become *the* tool to learn, tune, and deploy for many important domains, including healthcare, finance, education, and security [10, 19, 29, 51]. However, machine learning is not without its own limitations: countless works have demonstrated the fragility of models when in the presence of an adversary [12, 26, 36, 42, 48]. Across a variety of threat models, research has shown how adversaries fully control model outputs, by classifying school buses as ostriches [62], students as celebrities [56], or generating photos of synthetic, yet unsettlingly realistic, people [25].

This field of *adversarial machine learning* is rich with research into the exploitation of these models. While alarming to domains that have observed significant advancements as a result of machine learning (i.e., network intrusion detection, spam, malware, etc.), it is not clear yet whether these domains are as vulnerable as posited. This observation is rooted in the domain which exemplifies the end-to-end capability of deep learning: images. Influential works often use images as an empirical demonstration of their findings [12, 26, 36, 42, 48]. This has an implicit assumption on the underlying threat models; adversaries can manipulate features arbitrarily and independently. In other words, adversaries are assumed to have *full control* over the feature space and, more importantly, *all* input manipulations are equally permissible in the domain under investigation. While often bound (exclusively) by some self-imposed ℓ_p -norm (canonically used as a surrogate for human perception), there are constructs, rules, and other forms of *domain constraints* that many domains contain which images do not.

Domain constraints¹ describe relationships between features. For example, in network flow data, TCP flags can only be set for TCP flows in networks—having these flags for UDP would violate the semantics of the underlying phenomenon (network protocols). Constraints encode the maneuvers (i.e., perturbations) that are possible for an adversary when crafting adversarial examples. Yet, existing threat models broadly ignore this requirement, serving to generate examples that may or may not represent legitimate examples of

the domain. Thus, any vigilant system could simply discard non-compliant samples because they are manifestly adversarial—they do not represent a sample that could benignly exist. Such detectable adversarial examples, thus, pose no risk.

We argue in this paper that to properly assess the practical vulnerability of machine learning in a domain, the constraints that characterize the domain must be learned, incorporated, and demonstrated in attacks. Naturally, some domains contain incredibly rigid structures (e.g., binaries or networks) that could offer robustness against adversaries (that is, an *inability* to craft realizable adversarial examples), which is one of the central questions we investigate in this paper. By learning domain constraints, those who use machine learning can build accurate threat models and thus, properly assess realistic attack vectors.

Learning what the constraints are in arbitrary domains is a non-trivial process; domains can contain multiple layers of complex abstractions, frustrating any manual constraint identification through expertise. Fortunately, there are data-driven approaches for learning and encoding useful representations of constraints from areas within formal logic. One such method comes from the seminal work of Leslie Valiant on PAC learning (probably approximately correct learning) [67]. In this work, Valiant described a setting for learning boolean constraints (specifically, k -conjunctive normal form (CNF)) theories from data. Valiant’s constraint theory formulation and paired learning protocol provides a simple, yet exhaustive, mechanism for identifying constraints and, coincidentally, an elegant representation for integration into adversarial crafting algorithms.

In order to understand the robustness provided by domain constraints, we characterize the *worst-case adversary*. Specifically, the worst-case adversary is defined as one who is *least constrained*. Said formally, the number of possible observations rejected by a constraint theory is minimal. We describe the worst-case adversary by exploiting a theoretical property in our setting; a constraint theory is *sound* if the observations it certifies comply with the domain constraints. From this property, we show that sound constraint theories reduce to memorization of the training data, and how easing soundness yields generalization, with the worst-case adversary occurring under the *most general* (i.e., least constrained) constraint theory that can be learned.

In this paper, we explore adversarial examples with domain constraints by answering two fundamental questions: (1) *How would adversaries launch attacks in constrained domains?*, and (2) *Are constrained domains robust against adversarial examples?* We design our approach by leveraging frameworks within formal logic to learn constraints from data. Then, we modify an algorithm for constraint satisfaction, Davis–Putnam–Logemann–LoveLand (DPLL), to project adversarial examples onto a constraint-compliant space. Finally, we introduce a new adversarial crafting algorithm, the Constrained Saliency Projection (CSP): a blend of two popular adversarial crafting algorithms that, by design, aids DPLL in projection. We evaluate the efficacy of our approach on network intrusion detection and phishing datasets. From our investigation, we argue that incorporating domain constraints into threat models is *necessary* to produce realistic adversarial examples, and more

¹Note that the constraints discussed in this paper are different from *adversarial constraints*, which describe what an adversary seeks to achieve (commonly, a classification mismatch between model and human).

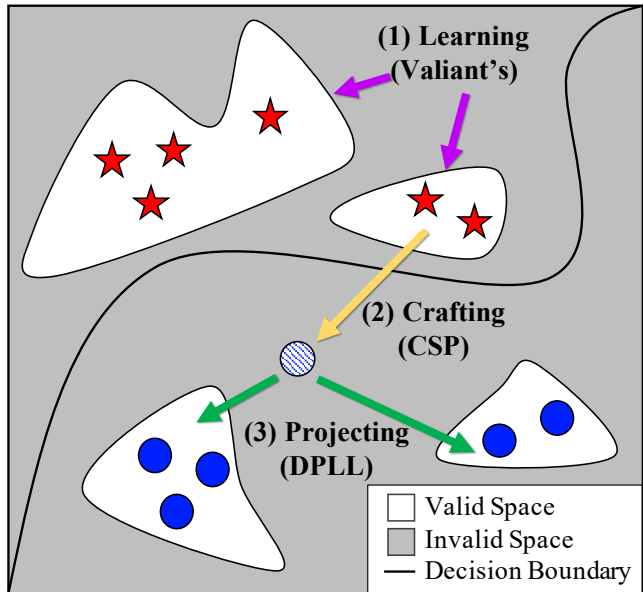


Figure 1: An Overview of Our Approach—Our approach consists of three steps: (1) learning the domain constraints, (2) crafting adversarial examples, and (3) projecting adversarial examples onto a constraint-compliant space.

importantly, constrained domains are naturally more robust to adversarial examples than unconstrained domains (e.g., images).

We contribute the following:

- (1) We formalize *domain constraints* in machine learning.
- (2) We prove *theoretical guarantees* for learning domain constraints in our setting. We describe when and why constraint theories are *sound* and *complete*, demonstrating an inherent trade-off between generalization and soundness.
- (3) We satisfy domain constraints by *projecting* non-realizable adversarial examples onto the space of valid inputs. We also introduce the Constrained Saliency Projection (CSP).
- (4) We demonstrate the robustness produced by domain constraints against worst-case adversaries in two diverse datasets. We observe that enforcing domain constraints can improve the robustness of a model substantially; in one experiment constraint enforcement restored model accuracy by 34%.

2 OVERVIEW

In order to measure the robustness of constrained domains against adversarial examples, we must build a new set of techniques. We can envision this process in three parts: (1) learning the domain constraints, (2) crafting adversarial examples, and (3) projecting adversarial examples onto a constraint-compliant space. A visualization of this approach is described in Figure 1.

Learning Constraints. In many domains, there are regions for which samples do not exist (e.g., UDP flows in the network domain do not have TCP flags). The structures and rules that define these regions may be complex and thus, we need a general approach to *learn* how domains are partitioned into valid and invalid regions.

We leverage an algorithm from PAC learning, Valiant’s algorithm, to learn these domain constraints in Section 4.2.

Crafting Adversarial Examples. After domain constraints have been learned, our approach can leverage *any* adversarial crafting algorithm. While there are many [12, 26, 42, 48] attacks in literature, we focus on PGD in Section 4.4 as it is considered to be the state-of-the-art for first-order adversaries. We will also consider a constraint-specific approach in Section 4.6.

Projecting Adversarial Examples. With the learned domain constraints and a set of adversarial examples, we must now enforce the constraints on the crafted adversarial examples. We do this by *projecting* the adversarial examples onto the constraint-compliant space (defined within some budget, as to preserve the goals of the adversary). Specifically, we manipulate features in constraint-noncompliant adversarial examples until they either satisfy the domain constraints or exceed the allotted budget. We augment a seminal solver for constraint satisfaction, DAVIS-PUTNAM-LOGEMAN-LOVELAND, to perform this projection in Section 4.5.

3 BACKGROUND

3.1 Threat Model

Adversarial Goals. Adversaries can have a variety of objectives, from reducing model confidence to misclassifying a sample as a particular target. Here, we focus on the former, that is, given a victim model f_θ with parameters θ , a sample e , label y , a self-imposed budget ϕ measured under some ℓ_p -norm, and a domain-dictated constraint theory T (which is our contribution), an adversary aims to solve the following optimization objective:

$$\begin{aligned} \arg \min_{\alpha} \quad & \|\alpha\|_p \\ \text{subject to} \quad & f_\theta(e + \alpha) \neq y, \\ & e + \alpha \in \mathcal{B}_\phi(e) \cap T \end{aligned} \quad (1)$$

Conceptually, the adversary searches within some norm-ball \mathcal{B} of radius ϕ around a sample e for a “small” change α to apply to e that yields the desirable model behavior (i.e., an *adversarial example*). In the context of computer security, this could translate to bypassing a network intrusion detection system.

“White-box” settings represent the strongest adversaries and characterize worst-case scenarios. Akin to insider threats, these adversaries have unfettered queries to the model, can observe its parameters, and can use its training data. From Equation 1, suppose f_θ describes the model of the defender, then white-box adversaries either have direct access to model parameters of f_θ or the training data used to learn f_θ . Practically speaking, such adversaries can produce adversarial examples with the tightest ℓ_p -norm constraints (i.e., the smallest budgets). “Gray-” and “Black-box” threat models are two other popular threat models that remove the degree to which an adversary has access to model parameters or training data. These limited adversaries usually require unique techniques for attacks to be successful [41, 46, 65].

In our work, we explore the efficacy of white-box adversaries when domain constraints are enforced. Specifically, the adversary seeks to minimize model *accuracy* (that is, the number of samples correctly classified over the total number of samples). Referring to Equation 1, the adversary computes samples classified as any

class $\hat{y} \neq y$ (where \hat{y} is the prediction). Under this objective, the adversary attempts to reduce the confidence an operator has in the predictions of a model.

3.2 Adversarial Machine Learning

We describe the two algorithms that serve as the basis for the algorithm used in our approach discussed later in Section 4.4.

Jacobian-based Saliency Map Approach (JSMA). The JSMA [48] is an iterative approach leveraging *saliency maps*: a heuristic applied to the Jacobian matrix of the model. For our work, the insightful component of the JSMA is that it selects a single feature to perturb per iteration (i.e., it optimizes over ℓ_0 -norms). This is especially important for security-critical domains as other $\ell_{p \neq 0}$ -norms are largely driven as surrogates for human perception, and do not apply to the studied domains.

Projected Gradient Descent (PGD). PGD², by Madry et al., is considered to be the state-of-the-art for first-order adversaries [42]. Similar to the Fast Gradient Sign Method [26], PGD iteratively multiplies a step-size α by the sign of the gradient of the loss to perturb the sample. As PGD has been proposed as a “universal adversary (among first-order approaches),” [42] we use it to evaluate the robustness of constraints against adversarial examples.

4 APPROACH

4.1 Preliminaries

We overview constraint learning and define the three algorithms we leverage for constraint learning, projection, and clustering.

Problem Statement. [52] provided one formulation for framing constraint learning as a concept-learning problem. We restate the relevant parts of the formalization for our work. Namely, we are given a domain $X = (X_1, \dots, X_n)$, where $X_i \subseteq \mathbb{Z}$ (i.e., we have n features where X_n denotes the unique values feature n can take), a space C of possible constraints (represented as k -CNF Boolean formulae defined over X), and a set E of collected observations. Our objective is to find a constraint theory T ($T \subseteq C$) such that T certifies all observations $e \in E$. We say T *certifies* e when all clauses $t \in T$ are satisfied by e . We say a clause t is *satisfied* when at least one literal in t is TRUE (where the features in e assign values to the literals in t). Conceptually, the collected observations E encode the structures or rules of the domain (i.e., T), that we seek to learn.

Valiant’s Algorithm. Valiant’s algorithm (Algorithm 1) is a general, exhaustive, generate-and-test algorithm for constraint learning [67]. The algorithm is initialized with a constraint theory T of all possible constraints over X (i.e., $T = C$). Then, for each observation $e \in E$, clauses that are not satisfied by e are removed from T . The algorithm terminates when E has been exhaustively processed. Valiant’s algorithm will converge to the correct solution, assuming E sufficiently represents the domain and is free of noise. Moreover, Valiant’s algorithm does not require any *negative examples* (that is, known observations that violate domain constraints, which are absent from popular machine learning datasets), which some constraint learning approaches require [23, 74]. Conceptually, T initially describes the *space of possible constraints* and, after

²The “projection” in PGD is unlike the “projection” used in this work through DPLL.

Input: observations E , boolean clauses T
Output: a conjunction of the remaining clauses T

```

1 for  $e \in E$  do
2   for  $c \in T$  do
3     remove  $c$  from  $T$  if  $e \not\models c$ 
4   end
5 end
6 return  $T$ 

```

Algorithm 1: Valiant’s Algorithm

Input: a domain X
Output: the space of possible constraints C

```

1  $P \leftarrow \{\mathcal{P}(X_i) \setminus \{\emptyset, X_i\} \mid X_i \in X\}$ 
2  $C \leftarrow \{P_1 \times \dots \times P_n, P_i \in P\}$ 
3  $C \leftarrow \text{RelaxToCNF}(C)$ 
4 return  $C$ 

```

Algorithm 2: Generating the Space of Possible Constraints

applying T and the set, E , of collected observations to Valiant’s algorithm, T will contain the set of constraints that are satisfied by *all* observations in E (in other words, the intersection of satisfied constraints across the observations in E).

To illustrate how Valiant’s algorithm operates, consider an example where a dataset contains samples with two binary features, $X_1 = \{x_1, \neg x_1\}$ and $X_2 = \{x_2, \neg x_2\}$. Then, C , the space of possible constraints is:

$$C = (x_1 \vee x_2) \wedge (x_1 \vee \neg x_2) \wedge (\neg x_1 \vee x_2) \wedge (\neg x_1 \vee \neg x_2)$$

If we initialize T (our target constraint theory) to C , and suppose E (our set of collected observations) consists of two observations $e_1 = (\text{FALSE}, \text{FALSE})$ and $e_2 = (\text{TRUE}, \text{TRUE})$, then Valiant’s algorithm first removes $(x_1 \vee x_2)$, and then removes $(\neg x_1 \vee \neg x_2)$ (as they are not satisfied by e_1 and e_2 , respectively). Our final constraint theory T is then $(x_1 \vee \neg x_2) \wedge (\neg x_1 \vee x_2)$. This example shows the thesis behind Valiant’s algorithm: *only constraints that have support from all observations are permissible*.

DPLL. For adversarial examples that do not comply with domain constraints, we use an algorithm from the constraint satisfaction community, DAVIS-PUTNAM-LOGEMAN-LOVELAND (DPLL) [17], to project adversarial examples onto the learned constraint theory returned by Valiant’s Algorithm. DPLL has some characteristics that make it ideal for our task, namely: (1) it accepts boolean formulae in CNF (which is the native form of the constraint theories learned by Valiant’s Algorithm), and (2) it is a *backtracking-based* search algorithm: DPLL iteratively builds candidate solutions for a given expression, which is a property we exploit, detailed later in Section 4.5. Further details about DPLL can be found in Appendix C.4

OPTICS. Later, we show how we model arbitrary data types as domain constraints. To support this generalization, we leverage a clustering algorithm, ORDERING POINTS TO IDENTIFY THE CLUSTERING STRUCTURE (OPTICS) [4]. OPTICS has two advantages over other clustering algorithms for our application, namely: (1) it scales to large sample sizes, and (2) it is *not* parameterized on specifying

the number of clusters. The second property is particularly important as parameterizing the number of clusters assumes a priori knowledge of the constraints before learning them in the first place.

4.2 Learning Constraints

Recall our problem statement: given a domain X , we first generate the space C of possible constraints, then, with a dataset E of samples, we use Valiant’s algorithm to prune constraints that do not comply with samples in our dataset (i.e., $T \subseteq C$). Valiant’s algorithm is elegant for binary features and the fact that it produces “hard” boolean constraints makes it attractive for encoding rigorous structures of domains. However, novel applications of machine learning seldom use binary features exclusively; categorical and continuous features (e.g., packet rates or word counts) are used in nearly every modern application of machine learning.

To address this limitation, there are two modifications that must be made: (1) how the space of possible constraints is generated, and (2) how to determine if a particular sample is certified by a constraint theory. We discuss these two modifications below.

The Space of Possible Constraints. For boolean-only constraint theories, the space of possible constraints is on the order of $\mathcal{O}(2^n)$, where n is the number of features. To account for categorical features, we can further generalize this bound to $\mathcal{O}(2^{n \cdot i})$ by considering a one-hot encoding, where i represents the largest cardinality of possible values among n features. This guides us on not only how to generate the space of constraints, but also how to modify Valiant’s algorithm to accept a richer representation of constraints.

Our approach, shown in Algorithm 2, is as follows: first, given a domain X , we compute a pseudo-power set P_i from the set X_i of unique values for feature i . P_i is a pseudo-power set as we remove the empty set (i.e., no value is valid for the feature) and X_i (which would allow the constraint to be trivially satisfied by any sample). We then perform the Cartesian product over P , which returns the set of all possible combinations of constraints; this is the input to Valiant’s algorithm (C). At this stage, C contains sets P_i of sets p_i , and so, we transform this representation to CNF (`RelaxToCNF`) by adding disjunctions between each $p_i \in P_i$ and, finally adding conjunctions between each $P_i \in C$.

To adapt Valiant’s algorithm to perform on a set-based representation of constraints (i.e., boolean *and* categorical variables), we redefine the \vdash operator (i.e., logical entailment); instead of evaluating whether or not a feature value causes a boolean assignment to be satisfied, we instead evaluate if it is a member of the set (i.e., $\not\models$ now operates as \notin , set membership, in Algorithm 1).

Consider the following example: suppose two features, X_1 and X_2 . Let X_1 be a boolean variable (encoded as $x_1 \in \{0, 1\}$) and let X_2 be a categorical variable that can take on one of three values (encoded as $x_2 \in \{A, B, C\}$). With our approach above, the space of possible constraints is then:

$$\begin{aligned}
C = & (x_1 \in \{0\} \vee x_2 \in \{A\}) \wedge (x_1 \in \{0\} \vee x_2 \in \{B\}) \\
& \dots \\
& \wedge (x_1 \in \{1\} \vee x_2 \in \{A, C\}) \wedge (x_1 \in \{1\} \vee x_2 \in \{B, C\})
\end{aligned}$$

If we initialize our target constraint theory T to C , and let E (our training data) consists of four samples $e_1 = (0, A)$, $e_2 = (0, B)$,

$e_3 = (1, B)$, and $e_4 = (1, C)$, then our objective is to guide Valiant’s algorithm to learn the following:

$$(x_1 \in \{0\} \wedge x_2 \in \{A, B\}) \vee (x_1 \in \{1\} \wedge x_2 \in \{B, C\})$$

Conceptually, we can imagine a case where X_1 describes a protocol (e.g., TCP or UDP), while X_2 describes a service (e.g., SSH, DNS, or NTP). Then, our target constraint theory T would be to learn that SSH can only be used with TCP, NTP can only be used with UDP, while DNS can be used with either TCP or UDP.

After running Valiant’s algorithm on this example, our final constraint theory T will be:

$$(x_1 \in \{0\} \vee x_2 \in \{B, C\}) \wedge (x_1 \in \{1\} \vee x_2 \in \{A, B\})$$

Using the distributive law, we see that this is precisely what we sought to learn. As a sanity check, we can see that the observations $(0, C)$ and $(1, A)$ violate T , which was our desired result.

Discretizing \mathbb{R} . While the framework above can express a richer expression of constraints than boolean theories, it cannot model variables that live within the domain of real numbers \mathbb{R} . However, modeling constraints that have inequalities such as $\{x \mid 0.25 \leq x \leq 0.80\}$ is non-trivial, as inferring the proper ranges for a given variable has no straightforward answer.

We are motivated to extend our set-based formulation of constraints to model continuous variables, as our generalization from the boolean domain \mathbb{B} to the domain of integers \mathbb{Z} has some ideal properties: (1) the set-based formulation can model constraints that are readily interpretable, (2) constraint-certification reduces to simple membership tests, (3) elegant integration into constraint learning algorithms, and, (4) gives a simple asymptotic bound to conceptualize the space of possible constraints. These properties are attractive and later we will show how our formulation can be integrated into adversarial crafting algorithms.

We leverage OPTICS to enable encoding of continuous features as discrete values. Here we express constraints with *sets of ranges* (e.g., $\{x \mid (0.25 \leq x_i < 0.50) \vee (0.75 \leq x_i < 1.00)\}$). Specifically, continuous features in samples are mapped to the bins and thereafter the associated constraints are learned as any other discrete feature. Later, when we project adversarial examples (discussed in Section 4.5), continuous features have their values set to the edge value closest to the origin of the perturbed value (i.e., a value that is projected from a higher number is set to the top of the bin range, and a lower number is set to the bottom of the range).

4.3 Theoretical Guarantees

In this section we define the properties that the learning process described above guarantees. When the full space of possible constraints is considered, our approach learns a constraint theory that is *sound* with respect to observations and domain constraints. Soundness guarantees that if a sample is certified by the constraint theory, then the sample complies with the domain constraints. The approach yields a sound constraint theory through Algorithm 2, generating the space of possible constraints (specifically the generation of the pseudo-power set). We first briefly describe our principal findings and later discuss formally when a constraint theory learned with our approach is sound and why.

Without loss of generality, consider that for all $X_i \in X$, $|X_i| = n$, that is, the number of unique values for all features is n . Then, the pseudo-power set³ contains sets of cardinality $1, \dots, k, \dots, (n - 1)$.

The clauses learned from sets of cardinality 1 (i.e., the cardinality of the literals in the clause is 1) represent the *most general* constraints, while clauses learned from sets of cardinality $n - 1$ represent the *least general* constraints (we show later that they represent rote memorization of the training data).

Let k bound the maximum cardinality considered when generating the pseudo-power set. Then, from our observations we gather that: (1) if $k = n - 1$ (i.e., the clauses generated contain literals of cardinality at most $n - 1$), the learned constraint theory is guaranteed to be sound, (2) if $k = 1$, the learned constraint theory is *maximally general*, and (3) for some k in-between 1 and n , there is a trade-off between the degree to which the learned constraint theory is sound (with respect to domain constraints at cardinality k) and how well it generalizes to unseen observations. Thus, k allows us to ease soundness and gain generalization, which we exploit in characterizing the worst-case adversary. In this way, k is the parameter that is used to tune the learned constraint theory from general to sound.

Next, we formally define the theoretical properties of our approach and show when and why they hold. Consider the following properties with respect to a constraint theory T and observations e :

- (1) **sound**: if T certifies e , then e complies with the domain constraints.
- (2) **complete**: for all possible observations e that comply with the domain constraints, T certifies e .

Recall (Section 4.1) that T certifies e when all clauses $t \in T$ are satisfied by e . A clause t is *satisfied* when at least one literal in t is TRUE (where the features in e assign values to the literals in t). Now, let Ξ represent the space of all possible observations. We can partition Ξ into two subspaces, Λ (the space of observations that comply with the domain constraints) and Ψ (the space of observations that do not comply with the domain constraints). Clearly, $\Lambda \cup \Psi = \Xi$ and $\Lambda \cap \Psi = \emptyset$. T is sound if it does not certify any observations from Ψ and T is complete if it certifies all observations from Λ .

When is T Complete? From the definition of complete, we can gather that T is axiomatically complete when T arbitrarily certifies *any* observation. Said alternatively, given that T is *not* complete if it does not certify all observations from Λ , T can be axiomatically complete when it certifies all observations, regardless if they come from Λ or Ψ . For example, the empty constraint theory $T = \emptyset$ is complete, as it will certify all possible observations $e \in \Lambda$ that comply with the domain constraints (as well as those that do not, i.e., $e \in \Psi$).

When is T Sound? From the definition of sound, we can gather that T is axiomatically sound when T does not certify *any* observations. Said differently, given that T is *not* sound if T certifies a single observation from Ψ , T can be axiomatically sound when it refuses to certify any observation. For example, when T equals the space of possible constraints C , T is axiomatically sound, as it will reject all possible observations $e \in \Psi$ that do not comply with the true domain constraints (as well as those that do comply, i.e., $e \in \Lambda$).

Properties of Our Approach. With the two settings for when T is sound or complete, we now turn to the setting investigated

³Recall that we generate a pseudo-power set by excluding the empty set \emptyset and the feature space itself, which correspond to sets of cardinality 0 and n , respectively.

in this paper. Specifically, we highlight some facts: (1) we have a set of observations E for which we know comply with the domain constraints (i.e., $E \subseteq \Lambda$), (2) we have no observations that do not comply with the domain constraints (i.e., $E \cap \Psi = \emptyset$), (3) Valiant’s algorithm can be initialized with the space of possible constraints (i.e., $T = C$), which entails: *T initially contains a superset of the domain constraints*. From (1), (3), and the fact that Valiant’s algorithm returns the intersection of satisfied constraints across the observations in E , we can derive the following: when T is initialized to C , *the learned constraint theory returned by Valiant’s algorithm is a superset of the domain constraints*.

Notably, the degree to which T remains a superset (and not equal to) of the domain constraints is a function of the quality of E in characterizing the underlying phenomena; as E approaches Λ , T converges on the domain constraints. In this way, Valiant’s algorithm prioritizes being sound over being complete.

Concretely, for any amount of observations in E , if T certifies a new observation, then it complies with the domain constraints (as T contains a superset of the domain constraints). However, if T does not certify a new observation that *does*, in fact, comply with the domain constraints, it is because this new observation failed to satisfy a clause $t^* \in T$ that should have been removed. Valiant’s algorithm would fail to remove the erroneous clause t^* if E did not contain a counter-example for t^* when learning T . Thus, unless $E = \Lambda$, T will not be complete (but T will always be sound).

Why is T Sound? The final piece in characterizing the worst-case adversary in our setting is rooted in analyzing what makes T sound. Specifically, T is sound through Algorithm 2: Generating the Space of Possible Constraints. Recall, we compute the Cartesian product of the pseudo-power set of unique values observed across all features. For each feature, the generated pseudo-power set can be decomposed as the union of the unique combinations of sets with cardinality $1, \dots, k, \dots, (n-1)$, where n represents the number of unique values observed for some feature i (i.e., $|X_i| = n$). For simplicity, consider only the clauses whose sets have cardinality $n - 1$. Trivially, this means that such clauses include all values for a given attribute, except one. Call this set of clauses C^* . In this setting, when E and C^* are passed into Valiant’s algorithm, *Valiant’s algorithm will return a learned theory T^* that is an exclusive encoding of E* . In other words, T^* will *only* certify E and nothing else (we formally prove this in Appendix A).

Note that, this is a useful fact as if $E = \Lambda$, then it would be desirable to learn a constraint theory that certified E and only E . However, when $E \subset \Lambda$ (as ostensibly all practical applications of machine learning do), then this reduces *learning* to *memorization* (this is analogous to *overfitting* in machine learning). From a learning perspective, this encourages us to bound the cardinality of pseudo-power set to be no greater than k , such that the learned constraint theory *generalizes*. Moreover, from an adversarial perspective, a constraint theory that *memorizes* the training data would require the adversary to craft adversarial examples that are precisely the training data itself. For any well-trained model, this means we already know where “adversarial examples” can exist: where the model produces errors on the training set. In other words, this characterizes the *best-case adversary*.

The Worst-Case Adversary. With these facts, we now characterize the *worst-case* adversary. Above, we observed how computing clauses with cardinalities of $n - 1$ results in constraint theories that certify the training data exclusively (that is, the total number of possible observations certified is at most $|E|$), which characterizes the *best-case adversary*. Thus, the *worst-case adversary* in our setting is one where the learned constraint theory is *most general*, in other words, certifies the *maximal* number of observations (which subsequently translates to certifying the maximal number of adversarial examples). To learn a theory that certifies the maximal number of observations, we set $k = 1$ when generating the pseudo-power set, which then results in clauses whose literals have cardinality 1 (we formally prove such constraint theories certify a maximal number of observations in Appendix A).

4.4 Crafting Adversarial Examples

On ℓ_p, ℓ_p -norms have been adopted by the academic community as the de facto standard for measuring a form of “adversarial constraints.” That is, it serves as a measurement of detectability as a surrogate for human perception (for image applications) or some arbitrary limitation on adversarial capabilities. For the former, it has been generally agreed upon that ℓ_2 or ℓ_∞ serve as better estimates of human perception. For the latter, adversarial capabilities are usually argued from a domain-specific perspective. For non-visual domains, we argue that the ℓ_0 norm is most representative of adversarial capabilities for two reasons: (1) distance across features in non-image data is not uniform; $\ell_{p \neq 0}$ -norms on varying data types and semantics bear no meaningful interpretation, and (2) for non-image domains, the degree to which an adversary can manipulate *every* feature yields little insight versus *what* features an adversary can manipulate.

Adversarial Constraints. Yet another important topic of discussion for applications of adversarial machine learning outside of images is: *what is the adversary trying to accomplish?* For images, this has been rooted in the use of ℓ_p -norms: there should be a misclassification between human and machine. For other domains, each have their own answer, e.g., consumer reviews should be read as containing positive sentiment by humans, yet classified as negative sentiment by machine (or vice-versa) [49]; malware should maintain its malicious behavior, post-perturbation [28, 35]; speech recognition systems should incorrectly map audio to commands versus what a human would hear [13], among other objectives. For our work, we follow similar intuitive objectives, that is, post-perturbation: malicious network flows must maintain their attack goals and phishing websites must mimic victim websites.

After defining *what* the goals of an adversary are, the next question is: *how do we know the adversary has met those goals?* For images and text, it has assumed to be self-evident; peers can inspect images produced by a crafting algorithm or read the altered text of a consumer review. While human-based verification is possible in some domains, in others (particularly those that are security-critical) it is not. For example, to validate that a network flow or a malware executable is malicious, then it must be replayed and its behavior observed in its respective domain. However, this may not always be possible; mapping back from a feature vector of an adversarial example to its original form may be non-trivial or outright

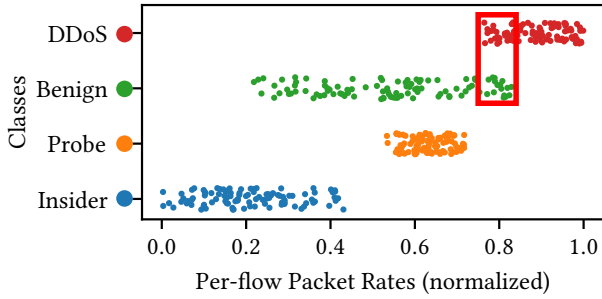


Figure 2: Encoding Adversarial Constraints — Distribution for normalized, per-flow PACKET RATES with classes from the NSL-KDD dataset. The region for the adversary attempting to classify DDoS traffic as BENIGN traffic, while maintaining the semantics of the attack, is shown in the rectangle.

impossible (network intrusion detection datasets may not always provide the packet captures used to build the dataset). Therefore, we need an approach that preserves the goals of an adversary when the original form of a sample cannot be rebuilt.

To address this limitation, we formulate and add an additional layer of “adversarial constraints” that encode class-specific behaviors. Specifically, we capture class-specific *feature bounds*, which are either: (1) the set of observations for categorical variables, or (2) the minima and maxima for continuous variables. We argue that the underlying behavior of a sample is preserved if it does not step outside of its bounds (which we hand validate). The intuition is straightforward: by staying within these bounds, then we produce adversarial examples with behaviors (as defined by feature values) that *have already been observed* for a particular class.

To illustrate this approach, consider Figure 2. Shown in this network intrusion detection example, there are four classes, DDoS, Benign, Probe, and Insider and each class has unique range of values for the Packet Rates feature. Suppose an adversary begins with a malicious DDoS sample and wishes to have it misclassified as Benign. Then, to preserve the underlying behavior of the sample, any perturbation to the DDoS sample must be between ~ 0.75 and ~ 1.0 . Naturally, the target region for the adversary is shown in the box, where the packet rates for DDoS and Benign overlap. We enforce adversarial constraints while generating adversarial examples as well as projecting them.

4.5 Projecting Adversarial Examples

The final step in our approach is to project some adversarial example e^* onto the constraint-compliant space described by the learned constraint theory T , as, if T does not certify e^* , then e^* is not adversarial at all, as it would not be *realizable* (as T encodes what is valid for a domain). This projection is non-trivial as there could be multiple features that do not comply with T and so, deciding which features to modify in e^* so that T certifies e^* could induce other features to become non-compliant, etc. Therefore, we need a mechanism that can efficiently project e^* as to comply with T .

This problem is isomorphic to constraint satisfaction problems; given a boolean expression T with some number of clauses $t \in T$,

we seek to find an assignment $\{\text{TRUE}, \text{FALSE}\}$ to each literal in t such that T is TRUE. For our work, we use the Davis-Putnam-Logemann-Loveland (DPLL) algorithm [17]. As discussed earlier in Section 4.1, DPLL has some properties that make it ideal for our task, particularly that it is a *backtracking-based* search algorithm.

DPLL is parameterized on H (shown in Algorithm 3 in Appendix C.4), a boolean theory with *partial* literal assignments (adapted to accept our set-based constraint representation, discussed in Section 4.2). We can exploit this fact by projecting an adversarial example e^* onto the space described by the learned constraint theory T . Specifically, for each clause t in T , we determine which clauses are satisfied with respect to value of features in e^* . If all clauses $t \in T$ are satisfied, then we simply return the adversarial example (as T certifies e^*). Otherwise, for each feature i in e^* , we record the number of clauses $t \in T$ satisfied by e_i^* .

Finally, we build H by allowing the bottom $\phi\%$ of literals to be unassigned while we assign the top $100 - \phi\%$ of literals to the corresponding feature values in e^* . Here, ϕ parameterizes: (1) the depth of the tree produced by DPLL (and thus its runtime), and (2) indirectly controls the likelihood e^* will still be misclassified (and thus, an adversarial example) after the assignment returned by DPLL is applied to e^* . To achieve (2), ϕ should be small to maintain the misclassification of e^* , yet large enough that DPLL has a sufficiently-sized search space to successfully project e^* onto T .

4.6 Improving Projection

In our evaluation, we find that adversarial examples produced by PGD often fail to be projected onto the constraint-compliant space described by T (within the allotted ϕ budget). Our hypothesis on why these projections failed stems from the fact that PGD optimizes over the ℓ_∞ norm, while the structure of the constraints and the budget used by DPLL may favor adversarial crafting algorithms that optimize over the ℓ_0 norm. With this hypothesis, we introduce our own ℓ_0 -based adversarial crafting algorithm that blends the iterative optimization of PGD with *saliency maps* from the JSMA.

The Constrained-Saliency Projection (CSP). The CSP is our approach. Like PGD, we consider a powerful adversary who can take multiple steps on the sign of the gradient of some loss function (or, in our case, the Jacobian of the model) and like the JSMA, the adversary computes *saliency maps* to determine the single most influential feature (and thus the feature to perturb), and unlike either, we project back onto a constraint-compliant space (described by T , our extracted constraint theory). Formally, we define the CSP as:

$$\begin{aligned} \mathbf{S} &= \text{SaliencyMap}(\hat{y}, \mathbf{J}(e^r)) \\ i &= \arg \max_j |S_j| \\ e_i^{r+1} &= e_i^r + \alpha \cdot \text{sgn}(S_i) \end{aligned}$$

where \mathbf{S} is the saliency map for a target⁴ class \hat{y} , \mathbf{J} is the Jacobian of a model with respect to the k -th perturbation of a sample e , i is a feature index, and α is the perturbation magnitude. We slightly tweak the definition for SaliencyMap that is originally proposed in [48]:

⁴We also consider an untargeted variant of the CSP where we set \hat{y} to the label y for sample e and use the negative of the Jacobian.

Dataset	# Samples	# Features	# Classes
NSL-KDD	$\approx 10^5$	11	5
Phishing	$\approx 10^4$	10	2

Table 1: Summary of Dataset Statistics

$$\text{SaliencyMap}_i(\hat{y}, \mathbf{J}) = \begin{cases} 0 & \text{if } \text{sgn} J_{\hat{y},i} = \text{sgn}(\sum_{j \neq \hat{y}} J_{j,i}) \\ J_{\hat{y},i} \cdot |\sum_{j \neq \hat{y}} J_{j,i}| & \text{otherwise} \end{cases}$$

where $J_{j,i}$ refers to the j th class and i th feature in the model Jacobian. This approach yields a subtle improvement; the formulation of the JSMA in [48] required a perturbation parameter that could be either positive or negative (which determined the heuristic used to build the saliency maps). However, our formulation for saliency maps allows the CSP to iteratively add or subtract from a feature i , depending on whichever is more advantageous for the adversary.

5 EVALUATION

With our techniques to learn and integrate domain constraints into the adversarial crafting process, we evaluate our approach on two diverse datasets. We ask the following:

- (1) Do known crafting algorithms violate domain constraints?
- (2) Do domain constraints provide robustness?

5.1 Experimental Setup & Datasets

Our experiments were performed on a Dell Precision T7600 with an Intel Xeon E5-2630 and a NVIDIA Geforce TITAN X. We used Cleverhans [45] for adversarial attacks and PyTorch [50] for building models. We defer to Appendix C for hyperparameters, architectures, and other miscellanea concerning our models. The experimental datasets are summarized in Table 1 and described below.

In the following figures, CSP and PGD refer to the attacks pre-projection, while the Constrained- variants show the results, post-projection, with DPLL and the learned domain constraints. We report the rate of invalid samples as the number of adversarial examples that do not comply with domain constraints over the total number of adversarial examples crafted. Model accuracy is measured as the number of adversarial examples classified correctly by the model over the total number of adversarial examples crafted. For constrained variants, samples that do not comply with domain constraints after projection are counted as correctly classified.

NSL-KDD. The NSL-KDD [63] is a subset of the seminal KDD Cup '99 network intrusion detection dataset, dating back to 1999. While the NIDS data is somewhat dated, the breadth and depth of the NSL-KDD makes it ideal for studying the effect of domain constraints. The dataset contains 125,973 samples for training and 22,544 for testing, representing four attacks and benign traffic.

As [1] demonstrates, many features in the NSL-KDD describe redundant information. Thus, we apply the same feature reduction techniques to the data to bring the feature space from 41 features down to 11. This had a minor impact on the accuracy of our models (i.e., from 77% down to 70%), yet drastically improved the scalability of learning domain constraints from the data.

Phishing. Phishing [16] is a dataset for identifying website phishing. The dataset contains *internal* and *external* features of a website, e.g., HTML versus WHOIS records. The features were extracted from 5,000 popular phishing websites and 5,000 legitimate webpages.

Moreover, [16] demonstrates that, among the original 48 features, only ten were necessary to maximize model accuracy. We use these ten suggested features to apply our constraint learning algorithms on and build our models from. As [16] claimed, we were able to achieve maximal model accuracy (i.e., above 94%) with ten features.

5.2 Learning Domain Constraints

Constraint Representation. Modern machine learning datasets often contain tens of thousands of samples and learned constraint theories can be equally as large (or even greater for some domains). Thus the runtime performance of the constraint generation and evaluation algorithms is important; we use a representation of domain constraints so that evaluation is efficient. Details on these optimizations are in Appendix C.5.

The Space of Constraints. Motivated by our theoretical analysis in Section 4.3, our evaluation characterizes the *worst-case adversary*. That is, our learned constraint theory T is maximally general in that it certifies the maximal number of observations (i.e., the threat surface of potential adversarial examples is maximal). To this end, we bound the pseudo-power set P , and therefore the literals in each clause, to have cardinality $k = 1$.

Constraints Learned From Our Datasets. After having generated clauses whose literals have cardinality $k = 1$, we pass C and the full datasets into Valiant’s algorithm. We find that the NSL-KDD, the network intrusion detection dataset, contained the most constraints at 5,330, while only 1,995 constraints were learned from Phishing, the phishing websites dataset. We will provide some introspection on the constraints learned from the NSL-KDD later in Section 6.

5.3 Crafting Adversarial Examples

For each dataset, we generate adversarial examples through both PGD and the CSP. Both algorithms apply a $0.01 \ell_\infty$ perturbation at each iteration (e.g., 35 iterations corresponds to a perturbation magnitude no greater than 0.35, roughly a third of the feature space) to continuous features. Perturbations to binary or categorical features are enforced to be -1 or 1 through one-hot encoding (as adversarial examples that report using 0.5 TCP for a Protocol feature are non-sensical). We compute results by generating adversarial examples over the test set and measure robustness through model accuracy.

5.4 Projecting Adversarial Examples

Selecting Features for DPLL to Perturb. Recall from Section 4.5, we first identify the feature values of adversarial examples that satisfy the fewest constraints (therein identifying the features that are most constrained by the domain). Intuitively, the heuristic we describe below is based on the following insight: if the most constrained features are perturbed, then the resultant adversarial example is likely to be rejected by the constraint theory. Thus, for each adversarial example, we identify the most constrained features and use DPLL to modify these features so that the sample is likely to be certified by the learned constraint theory.

Figure 3 shows clause satisfaction bar charts for Phishing and the NSL-KDD after 35 iterations of perturbations by the CSP and PGD. Recall that to use DPLL effectively, we wish to project constraint-noncompliant samples onto the constraint-compliant space with minimal sample modification under a ϕ budget. Additional information on the features can be found in Appendix C.3.

As the charts show, there are some features that satisfy significantly more clauses than others across the majority of samples. Because DPLL is parameterized on some allotted ϕ , this discrepancy suggests that we might use clause satisfaction as a heuristic to select features for DPLL to prioritize. In other words, we configure DPLL to prioritize projecting features whose values satisfy few clauses (as opposed to features whose values readily satisfy many clauses). We parameterize DPLL with an additional ϕ budget of 20% (i.e., DPLL will select no greater than the bottom 20% of features, as determined by the clause satisfaction bar charts, to project adversarial examples onto the learned constraint theory).

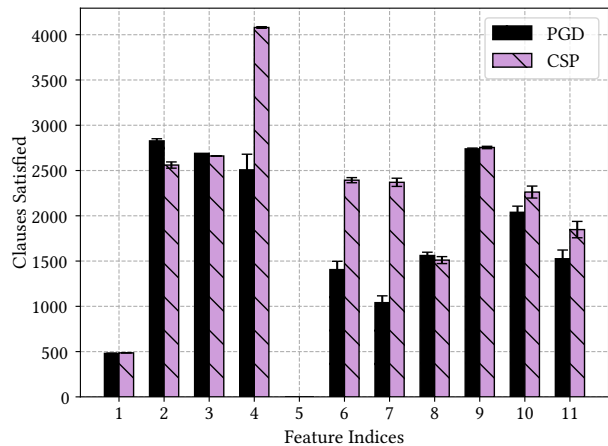
While this clause satisfaction heuristic is effective, other heuristics may improve DPLL success further. For instance, high variance in number of clauses satisfied by a feature across many samples could imply that the feature is highly salient towards constraints. We defer investigation of additional heuristics for future work.

Measuring the Efficacy of Constraints. Figure 4 illustrates the rate of invalid samples (that is, the number of constraint non-compliant adversarial examples over the total number crafted) and model accuracy as a function of the number of iterations used to craft adversarial examples.

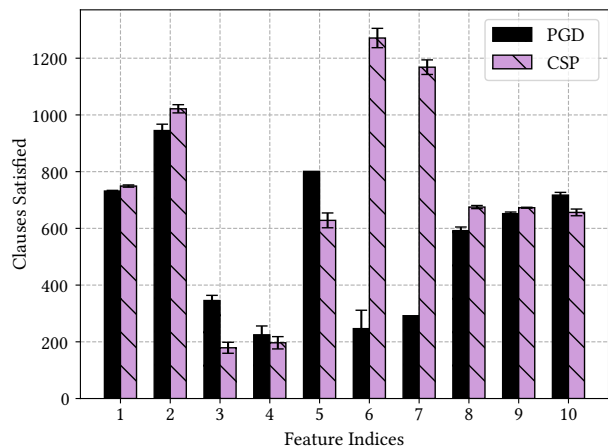
The rate of invalid samples (Figures 4a and 4b) answers our first evaluation question: *do the known crafting algorithms violate domain constraints?* Across both the NSL-KDD and Phishing, we observe that *at least 60%* of all adversarial examples produced by PGD violate the domain constraints when the number of iterations exceeds 10. In cases where domain constraints are violated, the adversarial examples produced are not realizable.

For our second evaluation question: *Do constraints add robustness?* The results suggest that domain constraints add robustness against adversarial examples. For example, we observe that even though DPLL was largely able to successfully project the adversarial examples produced by PGD when the number of iterations was small, many of the resultant constraint-compliant adversarial (i.e., CONSTRAINED-PGD) examples were correctly classified by the model. Notably, we observe how 34% of model accuracy is restored in the Phishing dataset (Figure 4d) once invalid examples produced by PGD are projected back onto a constraint-compliant space. On the NSL-KDD dataset, running PGD with many iterations produced additional examples that could not be projected into the constraint-compliant space, increasing the accuracy of the model.

Finally, we examine the applicability of CSP to crafting valid adversarial examples. The conservative nature of the CSP lends itself to producing adversarial examples that readily comply with domain constraints: at 10 iterations, only 10% of the examples produced by the CSP violated domain constraints in the worst case (compared to nearly 60% for PGD). Additionally, while many examples produced by PGD cannot be projected onto the constraint-compliant space (about 40% for the Phishing dataset), examples produced by CSP were successfully projected nearly 100% of the time. This suggests



(a) NSL-KDD

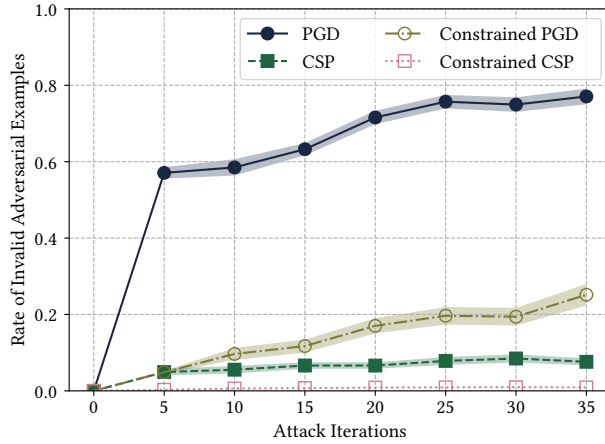


(b) Phishing

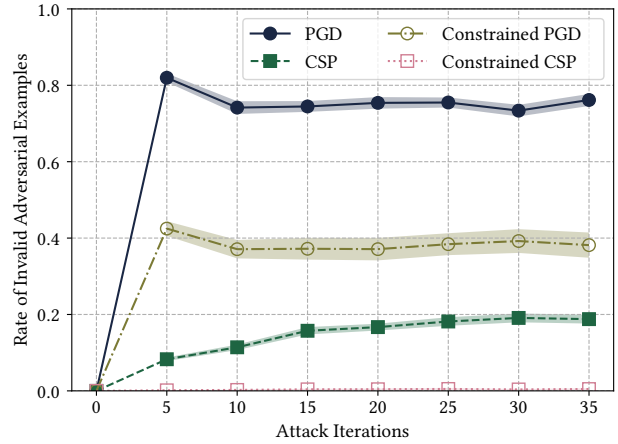
Figure 3: Clause Satisfaction Bar Chart—The mean number of clauses satisfied from the learned constraint theories on a per-feature basis for the adversarial examples produced by CSP and PGD. Error bars represent 95% C.I.

that saliency-based algorithms, as well as algorithms targeting an ℓ_0 norm, may be more readily applicable to constrained domains than gradient-based algorithms or those targeting ℓ_∞ . This is consistent with the structure of constraints and budget used by DPLL; PGD causes larger perturbations over ℓ_0 , which will likely violate more constraint clauses and frustrate projection.

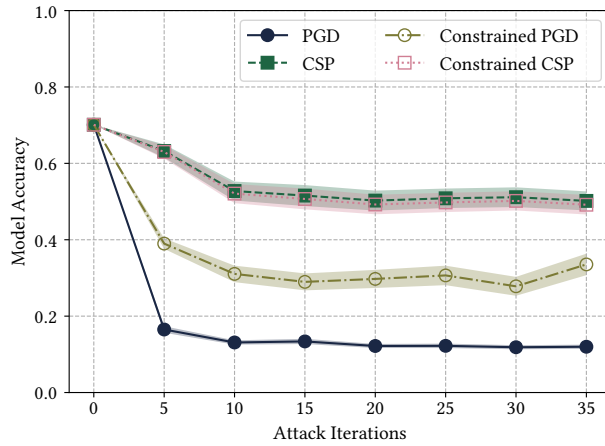
Takeaway. From our investigation, we highlight key takeaways: (A) *Crafting constraint-compliant adversarial examples is a necessarily different process than traditional crafting approaches.* Up to 82% of adversarial examples produced by PGD violated domain constraints. (B) *Constraints add robustness.* In the worst case, 34% of model accuracy was restored after projecting adversarial examples onto the learned constraint theory.



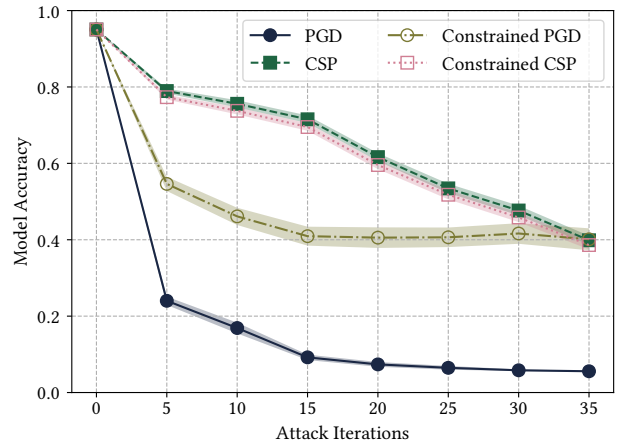
(a) NSL-KDD — Rate of Invalid Adversarial Examples



(b) Phishing — Rate of Invalid Adversarial Examples



(c) NSL-KDD — Model Accuracy



(d) Phishing — Model Accuracy

Figure 4: Crafting Adversarial Examples with Domain Constraints—Rate of invalid samples and model accuracy as a function of attack iterations (iterations add ± 0.01 to continuous features and ± 1 to categorical features). CSP and PGD refer to the attacks pre-projection, while Constrained variants demonstrate results post-projection with DPLL. Shaded regions represent 95% C.I.

The results demonstrate that crafting adversarial examples in constrained domains is a *necessarily* different process than those of unconstrained domains. Domain constraints have a tangible impact on the underlying threat surface as many of the threats produced by known crafting algorithms are not *realizable*. Perhaps most importantly, the relationships between features serve as a form of robustness to the known crafting algorithms.

5.5 Scalability

We next consider the scalability of our approach. Recall that Valiant’s Algorithm (Algorithm 1) checks each constraint against each observation, returning only constraints that certify all observations. Valiant’s algorithm, therefore, has time complexity $O(|E| \cdot |T|)$ (Note that $|T| = O(|C|)$). For clauses of cardinality $k = 1$, $|C| =$

Datasets	$ E $	$\prod X_i $	d	$\frac{d}{ E \cdot \prod X_i }$
NSL-KDD	1.5×10^5	1.0×10^4	180 s	1.2×10^{-7} s
Phishing	1.0×10^4	8.4×10^3	7 s	8.3×10^{-8} s
CICDDoS2019	2.5×10^6	1.3×10^4	4560 s	1.4×10^{-7} s
DREBIN [5] (<i>est.</i>)	1.2×10^5	5.6×10^5	8046 s	—
a9a [34] (<i>est.</i>)	4.6×10^4	7.6×10^6	39500 s	—
Mean				1.1×10^{-7} s

Table 2: Measured and estimated time to learn constraints

$\prod_{X_i \in X} |X_i|$, and the algorithm takes time $O(\prod |X_i|)$. Thus the combined runtime is $O(\prod |X_i| + |E| \cdot |T|) = O(|E| \cdot \prod |X_i|)$.

Next, we explore how the approach scales with real datasets. Table 2 shows, for each dataset, the number of unique samples $|E|$,

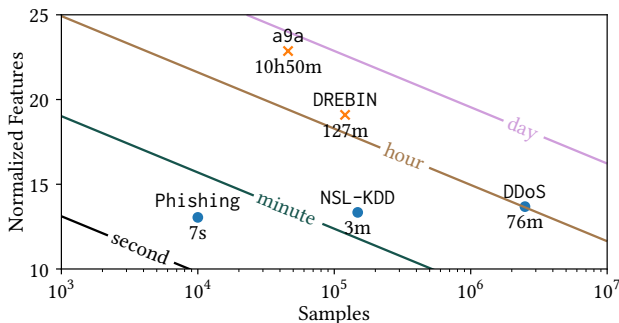


Figure 5: Scalability of constraint learning. Contours show time to learn constraints based on samples and features. Feature counts have been normalized ($\log_2 \prod |X_i|$) to approximate equivalent binary features. For comparison we superimpose actual and estimated runtimes of various datasets

the size of the power set and the total run time to execute the learning process. In addition to the NSL-KDD and Phishing datasets and to observe performance under large $|E|$, we measure performance on the large CICDDoS2019 dataset [55] which contains 2.5 million unique samples, after applying feature reduction techniques, as shown in [39], from a complex network environment. We also provide estimated performance on two additional datasets after feature reduction techniques inspired by literature.

Figure 5 visualizes the performance of the learning process over measured and estimated datasets. Here we show (1) the number of samples in the training data, and (2) the number of features. To allow comparison between datasets with differing classes per feature, we use a normalized feature count, which is the equivalent number of binary features which would yield the same $\prod |X_i|$. We superimpose actual and estimated performance numbers for comparison. From this, it can be seen that compute time scales linearly with the number of samples, but exponentially with the number of features. Because the number of samples in a training dataset should generally increase exponentially with the number of features (i.e., the curse of dimensionality [6]: the number of features should be $\mathcal{O}(\log |E|)$), the complexity of learning constraints on well-formed datasets can be roughly modeled as $\mathcal{O}(|E|^2)$. As previously noted, feature reduction techniques can further increase the tractability of high-dimensionality datasets without significantly lowering model accuracy. Additionally, further optimizations in the constraint learning routine might greatly improve throughput.

As a final note, recall our use of OPTICS for clustering continuous variables; we observed significant performance bottlenecks here. OPTICS computes pairwise distances between points that are within a parameterized ϵ neighborhood distance. For completeness, we set ϵ to ∞ , which yields a runtime of $\mathcal{O}(n^2)$. Depending on the number of samples, this can take *days* to determine the clusters alone (for comparison, once the clusters are identified, constraint learning can be done on the order of minutes). Supplementary experiments did show that OPTICS could approximate clusters fairly well with 1% randomly sampled subsets of the training data (e.g., for the NSL-KDD, out of the 18 clusters identified across features with the

Dataset	# Clauses	# Violations	% Violations
NSL-KDD	5,874	401	1.7%
Phishing	2,143	14	0.45%

Table 3: Constraint Violations from Test Set Observations

full training set, 16 clusters were consistently correctly identified with 1% randomly sampled subsets of the training set).

6 DISCUSSION

Projecting vs. Enforcing Constraints. One of the core components of the CSP is using DPLL to project adversarial examples onto the constraint compliant space, characterized by T . In preliminary experiments, we enforced T throughout the crafting process, that is, at any arbitrary iteration r , e^r was always a realizable adversarial example. However, we observed that, in some cases, the domain constraints would create “archipelagos” around inputs; any perturbations to an input were bound to small regions of the input space. Unconstrained domains, however, have input spaces that are more akin to supercontinents. This suggests that, for many domains deploying machine learning, the threat surface exposed by vanilla applications of adversarial machine learning is an overestimation (sometimes a large one) of the true, practical threat surface.

Robustness \cup Constraints. [53, 71] show two techniques for providing formal guarantees on model robustness (i.e., homogeneous predictions in a ℓ_∞ -norm ball). While these approaches have (at present) limitations that discourage practical deployment, they convincingly suggest that a model robust to adversaries is attainable. We note that there were no algorithms applied to our models to “secure” them, yet we observed tangible gains in model robustness from domain constraints. This suggests that the pairing of some form of model robustness with domain constraints may produce models that are highly challenging for an adversary to exploit. We present this as an opportunity for future work.

Addressing Concept Drift. Many applications of machine learning involve *non-stationary phenomena*; as the underlying phenomena changes over time, so does the space of observations that comply with the domain constraints. As a natural consequence of learning constraints from data, learning relevant constraint theories may necessitate: (1) identifying when concept drift has occurred, and (2) rectifying its effects on the learned constraint theory. We describe below several experiments that characterize the effects of concept drift on constraint learning.

Identifying concept drift is an unavoidable problem in machine learning, and there are approaches that can dynamically recognize concept drift and react to mitigate its effects (such as moving windows or detection thresholds) [22, 68, 69]. As a measurement of detecting concept drift, we investigated whether constraint theories learned exclusively from the training set would reject observations from the test set. Intuitively, this exercise is useful for two reasons: (1) it informs us if our approach overfits to a set of collected data (i.e., does Valiant’s algorithm *generalize?*), and (2) emulates what practical deployments of constraint learning would observe, given that datasets with a dedicated test set include new observations to approximate expected performance when deployed.

Our results, shown in Table 3 show a stark contrast in the violation rate between inputs from the test set and the adversarial examples crafted in our evaluation. These results confirm that: (1) Valiant’s algorithm does learn constraint theories that generalize well on unseen data, and, more importantly, (2) constraint violations can serve as an indicator of concept drift. For example, in a practical setting, network operators could use constraint violations as a “filter” for traffic flows that deserve attention and if the violation rate were to exceed some threshold, an indicator of concept drift through changes in the underlying traffic patterns.

Once concept drift has been identified, *rectifying* its effects can be challenging. Under the framework evaluated in this work, there are two facts on the effects of concept drift to a learned constraint theory: (1) new observations remove clauses that encode dated constraints, and (2) old observations could have removed clauses that encode constraints irrelevant at that time, but could be applicable at present (for example, a service could drop support for a particular protocol in future versions). In our setting, addressing dated constraints is straightforward: new observations could be used to remove the irrelevant constraints in a linear pass. However, re-adding constraints that were irrelevant in the past requires a more nuanced approach.

The naive approach would simply be to re-generate the universe of constraints and repeat the learning process in its entirety. However, this can be time-prohibitive for some domains, and so we are keen to use an approach where complete re-learning is not necessary. To this end, we are inspired by specific approach used in [69] to mitigate the effects of concept drift. Specifically, [69] stores concept descriptions and reuses them when a particular context appears. Thematically similar, we could first record the clauses removed for all observations in a training set. Then, if an observation is considered to be a dated representation of the domain (we could leverage domain expertise to identify such observations), we could simply re-add the removed clauses (insofar as no other observations would also remove those clauses). In this way, we can trade off repeating the learning process versus maintaining a record for the clauses removed for all samples.

The Quality of Learned Constraints. Ultimately the goal of this work is to develop constraints that reflect the true limitations of the domain. Historically, this has been the purview of domain experts. For example, Stolfo et al. developed a comprehensive constraints for network traffic [60]. Below, we show that by example the constraint theory learns constraints identified by humans (including those by Stolfo et al. and a number developed from our own experience with IP network protocols). We are exploring a more exhaustive analysis that systematically compares the specifications of IP protocols to the learned constraints.

To compare learned and human cultivated constraints, we formulate queries in the form of inputs that demonstrate constraints we would expect the constraint theory to learn. From our queries, we verified both obvious and subtle constraints, namely (1) if a TCP flow was terminated with REJ flag (i.e., through the source sending an initial SYN packet with the RST bit set), then the number of bytes sent in the flow must be 0 as, for the NSL-KDD, bytes measured in a flow was done post-handshake), and (2) SYN packets that have the same IP and port numbers for the source and destination fields,

flagged as “land” in the NSL-KDD, are never responded to. While the two above serve as examples of constraints from the TCP/IP protocol and domain experts respectively, the constraint theory also learned some attack-specific constraints, such as flows that had errors at some stage of the TCP handshake towards a specific service were distributed across destinations. After analyzing the kinds of flows that exhibited this property in the dataset, we observed that this was almost exclusively associated with probe attacks—this agrees with our understanding of probe attacks in that an adversary seeks to collect information of the services available in a network across destination hosts through a “heartbeat” mechanism, such as initiating connections to observe any form of response.

7 RELATED WORK

Learning in the Presence of Adversaries. The origins of adversarial machine learning are not explicitly known and are often disputed [7]. From our perspective, exploring the degree to which adversaries can influence learning algorithms begins in 1993 with Kearns et al. who formalize a worst-case data poisoning attack for any learning algorithm [32]. In 1997, [66] explores the efficacy of reinforcement algorithms in adversarial environments, with MINIMAX tables driving agent (and adversary) decisions.

The Rise of Deep Learning. With the rise in popularity in deep learning, adversarial scenarios were revisited [12, 26, 48, 62]. Many early works explored white-box, inference-time attacks via gradient-based algorithms. Shortly after, adversarial methods were translated from conceptual to practical, as works demonstrated how to produce adversarial examples in physical spaces, using stickers, glasses, and graffiti [9, 20, 36, 57]. Subsequently, adversarial machine learning was no longer exclusive to academia; it began to enter popular culture with discussions of fooling AI in magazine articles [24, 33, 43], demonstrating “DeepFakes” on television [38], and even displaying adversarial examples in museums [30].

In 2017 and 2018, there was a burst of adversarial machine learning research; transfer attacks (i.e., grey-box) [18, 37], black-box attacks on machine-learning-as-a-service platforms [8, 31, 46, 47], attacks by altering a single feature [61], data poisoning attacks (i.e., at training time) [2, 15], adversarial example detectors [11, 21, 27, 72], adversarially robust models through adversarial training [42], linear programming [71], and semidefinite relaxations [53, 59], among many other works. Seemingly every corner of machine learning involving some form of an adversary was explored.

Images and Beyond. As we motivated in Section 1, the majority of applications in adversarial machine learning have been in images. Recently, we have started to see applications in security domains, including malware [3, 28, 35], and network intrusion detection [40, 54, 58, 73]. These works all describe similar motivations: domains concerned with adversarial machine learning will likely not be exclusive to images. As canonical representatives of security, malicious software and network traffic are relevant phenomena to study. However, there are commonalities among the works that limit the applicability of the findings to practical deployments.

When perturbing inputs, these works exploit *domain “safe-spaces”*. For malware applications, the authors acknowledge that perturbing malware directly is incredibly challenging (without breaking it or removing its malicious purpose), therefore, perturbations are

limited to either appending bytes at the end of the binary [35] or only adding permissions to the list of required permissions for an application, in the context of Android malware [28]. These are two examples of “safe-space” perturbations: such manipulations guarantee that malicious behavior is preserved (and that the malware is still functional) by identifying regions that explicitly *avoid* domain constraints. This effectively reduces to manipulating image-like inputs, in that perturbations can be applied arbitrarily and independently.

For the works in network intrusion detection, some either ignore domain constraints [54, 73], or rely on domain expertise to identify what can and what cannot be perturbed [40, 58]. Specifically, [40] argues that insofar as the identified features are not perturbed, then the malicious behavior is preserved. Not unlike the malware scenarios, this models adversaries as being able to perturb arbitrarily and independently (just with a reduction to the allowable perturbation space, much like the one-pixel attack in [61]). However, [58] provides a method where all features can be perturbed with a sub-routine to enforce the domain constraints. The approach suffers from relying on expertise to identify the constraints correctly and is largely formulated for network intrusion detection systems.

While in this work we use images as a motivating example of an unconstrained domain, domain constraints can exist in images, depending on the subject of the image. Specifically, Chandrasekaran et al. identify domain constraints in images with domain expertise (as well as a data-driven approach via embeddings at intermediary layers of the model) [14]. They perform a complementary observation that adversarial crafting algorithms violate domain constraints, and, when domain constraints are enforced, model robustness is improved.

Where To? While we are moving closer to accurate threat models for diverse domains, we may ask, “What if such safe-spaces do not exist? What if the adversary is *required* to perturb in regions that may have effects on other features? Can such adversarial examples be realized?” We argue that these are fundamental questions for any domain that is keen to deploy machine learning.

8 CONCLUSION

This paper explored adversarial examples with *domain constraints*: relationships between features that encode the rules or structures of the underlying phenomena. We develop algorithms to learn constraint theories for given data distributions and integrate domain constraints into adversarial crafting processes. By representing domain constraints as logic clauses, we design a data-driven approach to learn the domain constraints across network intrusion detection and phishing datasets. We find that: (1) crafting adversarial examples in constrained domains is a *necessarily* different process than unconstrained domains; up to 82% of adversarial examples produced by PGD violated domain constraints, and (2) constrained domains are inherently more robust against adversarial examples; in one domain, 34% of model accuracy was restored after projecting adversarial examples onto the learned constraint theory. These findings suggest that the exploitable threat surface of models in constrained domains is likely narrower than previously understood.

ACKNOWLEDGMENTS

The authors would like to warmly thank the reviewers for their insightful feedback and Quinn Burke for his feedback on versions of this paper. This research was sponsored by the Combat Capabilities Development Command Army Research Laboratory and was accomplished under Cooperative Agreement Number W911NF-13-2-0045 (ARL Cyber Security CRA). The views and conclusions contained in this document are those of the authors and should not be interpreted as representing the official policies, either expressed or implied, of the Combat Capabilities Development Command Army Research Laboratory or the U.S. Government. The U.S. Government is authorized to reproduce and distribute reprints for Government purposes not withstanding any copyright notation here on. This material is based upon work supported by the National Science Foundation under Grant No. CNS-1805310. Any opinions, findings, and conclusions or recommendations expressed in this material are those of the author(s) and do not necessarily reflect the views of the National Science Foundation.

REFERENCES

- [1] O.Y. Al-Jarrah, A. Siddiqui, M. Elsalamouny, P.D. Yoo, S. Muhaidat, and K. Kim. Machine-Learning-Based Feature Selection Techniques for Large-Scale Network Intrusion Detection. In *2014 IEEE 34th International Conference on Distributed Computing Systems Workshops*, pages 177–181, Madrid, Spain, June 2014. IEEE.
- [2] Scott Alfeld, Xiaojin Zhu, and Paul Barford. Data Poisoning Attacks against Autoregressive Models. In *Proceedings of the Thirtieth AAAI Conference on Artificial Intelligence*, AAAI’16, pages 1452–1458. AAAI Press, 2016. event-place: Phoenix, Arizona.
- [3] Hyrum S Anderson, Anant Kharkar, and Bobby Filar. Evading Machine Learning Malware Detection. page 6.
- [4] Mihael Ankerst, Markus M. Breunig, Hans-Peter Kriegel, and Jörg Sander. OPTICS: Ordering Points to Identify the Clustering Structure. In *Proceedings of the 1999 ACM SIGMOD International Conference on Management of Data*, SIGMOD ’99, pages 49–60, New York, NY, USA, 1999. Association for Computing Machinery. event-place: Philadelphia, Pennsylvania, USA.
- [5] Daniel Arp, Michael Spreitzenbarth, Malte Hübner, Hugo Gascon, and Konrad Rieck. Drebin: Effective and Explainable Detection of Android Malware in Your Pocket. In *Proceedings 2014 Network and Distributed System Security Symposium*, San Diego, CA, 2014. Internet Society.
- [6] R E Bellman. *Adaptive Control Processes: A Guided Tour*. 1961.
- [7] Battista Biggio and Fabio Roli. Wild patterns: Ten years after the rise of adversarial machine learning. *Pattern Recognition*, 84:317–331, 2018. Publisher: Elsevier.
- [8] Wieland Brendel, Jonas Rauber, and Matthias Bethge. Decision-based adversarial attacks: Reliable attacks against black-box machine learning models. *arXiv preprint arXiv:1712.04248*, 2017.
- [9] Tom B Brown, Dandelion Mané, Aurko Roy, Martin Abadi, and Justin Gilmer. Adversarial patch. *arXiv preprint arXiv:1712.09665*, 2017.
- [10] A. L. Buczak and E. Guven. A Survey of Data Mining and Machine Learning Methods for Cyber Security Intrusion Detection. *IEEE Communications Surveys Tutorials*, 18(2):1153–1176, 2016.
- [11] Nicholas Carlini and David Wagner. Adversarial examples are not easily detected: Bypassing ten detection methods. In *Proceedings of the 10th ACM Workshop on Artificial Intelligence and Security*, pages 3–14, 2017.
- [12] Nicholas Carlini and David Wagner. Towards evaluating the robustness of neural networks. In *2017 IEEE Symposium on Security and Privacy (SP)*, pages 39–57. IEEE, 2017.
- [13] Nicholas Carlini and David Wagner. Audio adversarial examples: Targeted attacks on speech-to-text. In *2018 IEEE Security and Privacy Workshops (SPW)*, pages 1–7. IEEE, 2018.
- [14] Varun Chandrasekaran, Brian Tang, Nicolas Papernot, Kassem Fawaz, Somesh Jha, and Xi Wu. Rearchitecting Classification Frameworks For Increased Robustness, 2019. _eprint: 1905.10900.
- [15] Xinyun Chen, Chang Liu, Bo Li, Kimberly Lu, and Dawn Song. *Targeted Backdoor Attacks on Deep Learning Systems Using Data Poisoning*. 2017. _eprint: 1712.05526.
- [16] Kang Leng Chiew, Choon Lin Tan, KokSheik Wong, Kelvin S.C. Yong, and Wei King Tiong. A new hybrid ensemble feature selection framework for machine learning-based phishing detection system. *Information Sciences*, 484:153–166, May 2019.

- [17] Martin Davis and Hilary Putnam. A Computing Procedure for Quantification Theory. *J. ACM*, 7(3):201–215, July 1960. Place: New York, NY, USA Publisher: Association for Computing Machinery.
- [18] Yinpeng Dong, Tianyu Pang, Hang Su, and Jun Zhu. Evading defenses to transferable adversarial examples by translation-invariant attacks. In *Proceedings of the IEEE Conference on Computer Vision and Pattern Recognition*, pages 4312–4321, 2019.
- [19] Andre Esteva, Alexandre Robicquet, Bharath Ramsundar, Volodymyr Kuleshov, Mark DePristo, Katherine Chou, Claire Cui, Greg Corrado, Sebastian Thrun, and Jeff Dean. A guide to deep learning in healthcare. *Nature Medicine*, 25(1):24–29, January 2019.
- [20] Kevin Eykholt, Ivan Evtimov, Earlene Fernandes, Bo Li, Amir Rahmati, Chaowei Xiao, Atul Prakash, Tadayoshi Kohno, and Dawn Song. Robust physical-world attacks on deep learning visual classification. In *Proceedings of the IEEE Conference on Computer Vision and Pattern Recognition*, pages 1625–1634, 2018.
- [21] Reuben Feinman, Ryan R Curtin, Saurabh Shintre, and Andrew B Gardner. Detecting adversarial samples from artifacts. *arXiv preprint arXiv:1703.00410*, 2017.
- [22] João Gama, Pedro Medas, Gladys Castillo, and Pedro Rodrigues. Learning with Drift Detection. In Ana L. C. Bazzan and Sofiane Labidi, editors, *Advances in Artificial Intelligence – SBIA 2004*, pages 286–295, Berlin, Heidelberg, 2004. Springer Berlin Heidelberg.
- [23] Pranav Garg, Christof Löding, P. Madhusudan, and Daniel Neider. ICE: A Robust Framework for Learning Invariants. In Armin Biere and Roderick Bloem, editors, *Computer Aided Verification*, pages 69–87, Cham, 2014. Springer International Publishing.
- [24] Dave Gershgorn. *Fooling the machine*. Popular Science, April 2019. Publication Title: Popular Science.
- [25] Ian Goodfellow, Jean Pouget-Abadie, Mehdi Mirza, Bing Xu, David Warde-Farley, Sherjil Ozair, Aaron Courville, and Yoshua Bengio. Generative adversarial nets. In *Advances in neural information processing systems*, pages 2672–2680, 2014.
- [26] Ian J Goodfellow, Jonathon Shlens, and Christian Szegedy. Explaining and harnessing adversarial examples. *arXiv preprint arXiv:1412.6572*, 2014.
- [27] Kathrin Grosse, Praveen Manoharan, Nicolas Papernot, Michael Backes, and Patrick McDaniel. On the (statistical) detection of adversarial examples. *arXiv preprint arXiv:1702.06280*, 2017.
- [28] Kathrin Grosse, Nicolas Papernot, Praveen Manoharan, Michael Backes, and Patrick McDaniel. Adversarial examples for malware detection. In *European Symposium on Research in Computer Security*, pages 62–79. Springer, 2017.
- [29] JB Heaton, Nicholas G Polson, and Jan Hendrik Witte. Deep learning in finance. *arXiv preprint arXiv:1602.06561*, 2016.
- [30] Natashah Hitti. *Science Museum curator picks five designs for a driverless future*. Dezeen, July 2019. Publication Title: Dezeen.
- [31] Andrew Ilyas, Logan Engstrom, Anish Athalye, and Jessy Lin. Black-box adversarial attacks with limited queries and information. *arXiv preprint arXiv:1804.08598*, 2018.
- [32] Michael Kearns and Ming Li. Learning in the presence of malicious errors. *SIAM Journal on Computing*, 22(4):807–837, 1993. Publisher: SIAM.
- [33] Nicole Kobie. *To cripple AI, hackers are turning data against itself*. WIRED UK, September 2018. Publication Title: WIRED.
- [34] Ron Kohavi. Scaling up the Accuracy of Naive-Bayes Classifiers: A Decision-Tree Hybrid. In *Proceedings of the Second International Conference on Knowledge Discovery and Data Mining, KDD’96*, pages 202–207. AAAI Press, 1996. event-place: Portland, Oregon.
- [35] Bojan Kolosnjaji, Ambra Demontis, Battista Biggio, Davide Maiorca, Giorgio Giacinto, Claudia Eckert, and Fabio Roli. Adversarial malware binaries: Evading deep learning for malware detection in executables. In *2018 26th European Signal Processing Conference (EUSIPCO)*, pages 533–537. IEEE, 2018.
- [36] Alexey Kurakin, Ian Goodfellow, and Samy Bengio. Adversarial examples in the physical world. *arXiv preprint arXiv:1607.02533*, 2016.
- [37] Alexey Kurakin, Ian Goodfellow, and Samy Bengio. Adversarial machine learning at scale. *arXiv preprint arXiv:1611.01236*, 2017.
- [38] Kalev Leetaru. *What Happens When Television News Gets The Deep Fake Treatment?* Forbes Magazine, May 2019. Publication Title: Forbes.
- [39] Junhong Li. DETECTION OF DDOS ATTACKS BASED ON DENSE NEURAL NETWORKS, AUTOENCODERS AND PEARSON CORRELATION COEFFICIENT. page 89.
- [40] Zilong Lin, Yong Shi, and Zhi Xue. *IDS-GAN: Generative Adversarial Networks for Attack Generation against Intrusion Detection*. 2018. _eprint: 1809.02077.
- [41] Yanpei Liu, Xinyun Chen, Chang Liu, and Dawn Song. Delving into transferable adversarial examples and black-box attacks. *arXiv preprint arXiv:1611.02770*, 2016.
- [42] Aleksander Madry, Aleksandar Makelov, Ludwig Schmidt, Dimitris Tsipras, and Adrian Vladu. Towards deep learning models resistant to adversarial attacks. *arXiv preprint arXiv:1706.06083*, 2017.
- [43] Kimberley Mok. *Google Develops ‘Adversarial Example’ Images that Fool Both Humans and Computers*. The New Stack, May 2018. Publication Title: The New Stack.
- [44] Stephen Muggleton. Optimal layered learning: A PAC approach to incremental sampling. In Klaus P. Jantke, Shigenobu Kobayashi, Etsuji Tomita, and Takashi Yokomori, editors, *Algorithmic Learning Theory*, pages 37–44, Berlin, Heidelberg, 1993. Springer Berlin Heidelberg.
- [45] Nicolas Papernot, Ian Goodfellow, Ryan Sheatsley, Reuben Feinman, and Patrick McDaniel. cleverhans v1.0.0: an adversarial machine learning library. *arXiv preprint arXiv:1610.00768*, 2016.
- [46] Nicolas Papernot, Patrick McDaniel, and Ian Goodfellow. *Transferability in Machine Learning: from Phenomena to Black-Box Attacks using Adversarial Samples*. 2016. _eprint: 1605.07277.
- [47] Nicolas Papernot, Patrick McDaniel, Ian Goodfellow, Somesh Jha, Z Berkay Celik, and Ananthram Swami. Practical black-box attacks against machine learning. In *Proceedings of the 2017 ACM on Asia conference on computer and communications security*, pages 506–519, 2017.
- [48] Nicolas Papernot, Patrick McDaniel, Somesh Jha, Matt Fredrikson, Z Berkay Celik, and Ananthram Swami. The limitations of deep learning in adversarial settings. In *2016 IEEE European symposium on security and privacy (EuroS&P)*, pages 372–387. IEEE, 2016.
- [49] Nicolas Papernot, Patrick McDaniel, Ananthram Swami, and Richard Harang. Crafting adversarial input sequences for recurrent neural networks. In *MILCOM 2016-2016 IEEE Military Communications Conference*, pages 49–54. IEEE, 2016.
- [50] Adam Paszke, Sam Gross, Francisco Massa, Adam Lerer, James Bradbury, Gregory Chanan, Trevor Killeen, Zeming Lin, Natalia Gimelshein, Luca Antiga, Alban Desmaison, Andreas Kopf, Edward Yang, Zachary DeVito, Martin Raison, Alykhan Tejani, Sasank Chilamkurthy, Benoit Steiner, Lu Fang, Junjie Bai, and Soumith Chintala. PyTorch: An Imperative Style, High-Performance Deep Learning Library. In H. Wallach, H. Larochelle, A. Beygelzimer, F. d’textquotesingle Alch -Buc, E. Fox, and R. Garnett, editors, *Advances in Neural Information Processing Systems 32*, pages 8024–8035. Curran Associates, Inc., 2019.
- [51] Stefan A. D. Popenici and Sharon Kerr. Exploring the impact of artificial intelligence on teaching and learning in higher education. *Research and Practice in Technology Enhanced Learning*, 12(1):22, November 2017.
- [52] Luc De Raedt, Andrea Passerini, and Stefano Teso. Learning Constraints from Examples. page 6.
- [53] Aditi Raghunathan, Jacob Steinhardt, and Percy Liang. Certified defenses against adversarial examples. *arXiv preprint arXiv:1801.09344*, 2018.
- [54] Maria Rigaki. Adversarial Deep Learning Against Intrusion Detection Classifiers. 2017.
- [55] I. Sharafaldin, A. H. Lashkari, S. Hakak, and A. A. Ghorbani. Developing Realistic Distributed Denial of Service (DDoS) Attack Dataset and Taxonomy. In *2019 International Carnahan Conference on Security Technology (ICCST)*, pages 1–8, 2019.
- [56] Mahmood Sharif, Sruti Bhagavatula, Lujo Bauer, and Michael K Reiter. Accessorize to a crime: Real and stealthy attacks on state-of-the-art face recognition. In *Proceedings of the 2016 ACM SIGSAC conference on computer and communications security*, pages 1528–1540, 2016.
- [57] Mahmood Sharif, Sruti Bhagavatula, Lujo Bauer, and Michael K Reiter. A general framework for adversarial examples with objectives. *ACM Transactions on Privacy and Security (TOPS)*, 22(3):1–30, 2019. Publisher: ACM New York, NY, USA.
- [58] Ryan Sheatsley, Nicolas Papernot, Michael Weisman, Gunjan Verma, and Patrick McDaniel. Adversarial Examples in Constrained Domains. *arXiv:2011.01183 [cs]*, November 2020. arXiv: 2011.01183.
- [59] Jacob Steinhardt, Pang Wei Koh, and Percy Liang. Certified Defenses for Data Poisoning Attacks. In *Proceedings of the 31st International Conference on Neural Information Processing Systems, NIPS’17*, pages 3520–3532, Red Hook, NY, USA, 2017. Curran Associates Inc. event-place: Long Beach, California, USA.
- [60] S.J. Stolfo, Wei Fan, Wenke Lee, A. Prodromidis, and P.K. Chan. Cost-based modeling for fraud and intrusion detection: results from the JAM project. In *Proceedings DARPA Information Survivability Conference and Exposition. DISCEX’00*, volume 2, pages 130–144 vol.2, 2000.
- [61] Jiawei Su, Danilo Vasconcellos Vargas, and Kouichi Sakurai. One pixel attack for fooling deep neural networks. *IEEE Transactions on Evolutionary Computation*, 23(5):828–841, 2019. Publisher: IEEE.
- [62] Christian Szegedy, Wojciech Zaremba, Ilya Sutskever, Joan Bruna, Dumitru Erhan, Ian Goodfellow, and Rob Fergus. *Intriguing properties of neural networks*. 2013. _eprint: 1312.6199.
- [63] M. Tavallae, E. Bagheri, W. Lu, and A. A. Ghorbani. A detailed analysis of the KDD CUP 99 data set. In *2009 IEEE Symposium on Computational Intelligence for Security and Defense Applications*, pages 1–6, 2009.
- [64] Kevin Thompson, Gregory J Miller, and Rick Wilder. Wide-area Internet traffic patterns and characteristics. *IEEE network*, 11(6):10–23, 1997. Publisher: IEEE.
- [65] Florian Tram r, Nicolas Papernot, Ian Goodfellow, Dan Boneh, and Patrick McDaniel. The space of transferable adversarial examples. *arXiv preprint arXiv:1704.03453*, 2017.
- [66] William Uther and Manuela Veloso. Adversarial reinforcement learning. Technical report, Tech. rep., Carnegie Mellon University. Unpublished, 1997.
- [67] L.G. Valiant. A Theory of the Learnable. *Communications of the ACM*, 27(11):1134–1142, 1984.

- [68] Geoffrey I Webb, Roy Hyde, Hong Cao, Hai Long Nguyen, and Francois Petitjean. Characterizing concept drift. *Data Mining and Knowledge Discovery*, 30(4):964–994, 2016. Publisher: Springer.
- [69] Gerhard Widmer and Miroslav Kubat. Learning in the presence of concept drift and hidden contexts. *Machine learning*, 23(1):69–101, 1996. Publisher: Springer.
- [70] Carey Williamson. Internet traffic measurement. *IEEE internet computing*, 5(6):70–74, 2001. Publisher: IEEE.
- [71] Eric Wong and Zico Kolter. Provable defenses against adversarial examples via the convex outer adversarial polytope. In *International Conference on Machine Learning*, pages 5286–5295, 2018.
- [72] Weilin Xu, David Evans, and Yanjun Qi. Feature squeezing: Detecting adversarial examples in deep neural networks. *arXiv preprint arXiv:1704.01155*, 2017.
- [73] K. Yang, J. Liu, C. Zhang, and Y. Fang. Adversarial Examples Against the Deep Learning Based Network Intrusion Detection Systems. In *MILCOM 2018 - 2018 IEEE Military Communications Conference (MILCOM)*, pages 559–564, 2018.
- [74] He Zhu, Stephen Magill, and Suresh Jagannathan. A Data-Driven CHC Solver. *SIGPLAN Not.*, 53(4):707–721, June 2018. Place: New York, NY, USA Publisher: Association for Computing Machinery.

A THE WORST-CASE ADVERSARY

We call a constraint theory T *strict* when T *only* certifies the observations E from which T was learned; any other observation e^* that is not a member of E is rejected. Secondly, we call T *general* when it certifies a *maximum* number of observations (while containing a non-zero number of clauses).

We will now show that, in the setting described in this paper, the *most strict* constraint theories are those whose clauses have literals of cardinality $n - 1$ (recall, literals in our setting are sets), where n describes the number of unique values observed for a given attribute in the set of collected observations E . Such constraint theories describe the *best-case* adversary, as the adversary must produce adversarial examples that are precise copies of collected observations E .

Conversely, the *most general* constraint theories are those whose clauses have literals of cardinality 1. These constraint theories characterize the *worst-case* adversary, as such constraint theories certify the *maximum* number of observations among all constraint theories learned by considering literals with cardinalities from 1 to $n - 1$. Let ψ_k be the set of observations rejected by constraint theories T_k whose clauses contain literals with cardinality k . We will now show: $\psi_1 \subseteq \dots \subseteq \psi_k \subseteq \dots \subseteq \psi_{n-1}$

An Illustrative Domain. Consider the visualization in Figure 6 of some set of collected observations E (shaded in gray).

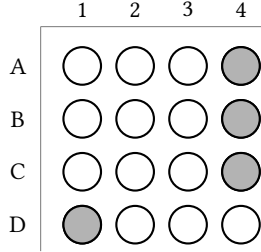


Figure 6: Domain and collected observations E —In the considered domain, there are two features x_1 and x_2 whose observations can take values $\{A, B, C, D\}$ and $\{1, 2, 3, 4\}$, respectively. The grey circles represent the set of collected observations E .

In this domain, there are two features: x_1 , which can take values $\{A, B, C, D\}$, and x_2 , which can take values $\{1, 2, 3, 4\}$. From E , we observe that if some observation e has value $x_1 = D$, then $x_2 = 1$, otherwise if $x_1 \neq D$, then $x_2 = 4$.

Next, we will consider the output of Algorithm 2, generating the space of possible of constraints, for literals of cardinality $k = 1, 2$, and $n - 1 = 3$. For clarity, a single clause will be written as $(\{\alpha\} \vee \{\beta\})$, where α represents at least one and at most three elements from x_1 (i.e., $\{A, B, C, D\}$), and β represents at least one and at most three elements from x_2 (i.e., $\{1, 2, 3, 4\}$).

$k = 1$. Let us consider the space of possible constraints for clauses generated with literals of cardinality $k = 1$:

$$\begin{aligned} & (\{A\} \vee \{1\}) \wedge (\{A\} \vee \{2\}) \wedge (\{A\} \vee \{3\}) \wedge (\{A\} \vee \{4\}) \wedge \\ & (\{B\} \vee \{1\}) \wedge (\{B\} \vee \{2\}) \wedge (\{B\} \vee \{3\}) \wedge (\{B\} \vee \{4\}) \wedge \\ & (\{C\} \vee \{1\}) \wedge (\{C\} \vee \{2\}) \wedge (\{C\} \vee \{3\}) \wedge (\{C\} \vee \{4\}) \wedge \\ & (\{D\} \vee \{1\}) \wedge (\{D\} \vee \{2\}) \wedge (\{D\} \vee \{3\}) \wedge (\{D\} \vee \{4\}) \end{aligned}$$

After applying Valiant’s algorithm to these constraints with our set of collected observations E , the resultant learned constraint theory is then:

$$T = (\{D\} \vee \{4\})$$

As we described above, our worst-case adversary is one who crafts adversarial examples for a constraint theory that is *most general*, among all possible learned constraint theories in our setting. Consider the learned constraint theory $T = (\{D\} \vee \{4\})$; this constraint theory will certify any observation e whose values are either (D, \cdot) or $(\cdot, 4)$ (where \cdot denotes any value from the domain of the respective attribute). From Figure 6, we can see that, out of the 16 possible instances in our exemplar domain, seven are accepted and nine are rejected, that is, $|\psi_1| = 9$. Now, we draw a “reject” box in red, respectively, shown in Figure 7.

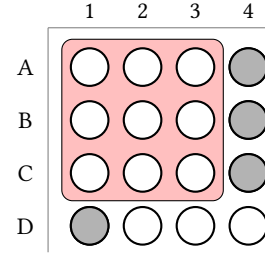


Figure 7: Reject space for $k = 1$ —For literals whose cardinality k is 1, the learned constraint theory $T = (\{D\} \vee \{4\})$ rejects any observation from the red box.

Reject boxes can be derived by inverting each individual clause and applying De Morgan’s law. For example, the reject box associated with clause $(\{D\} \vee \{4\})$ would be $\overline{(\{D\} \vee \{4\})} = \overline{(\{D\})} \wedge \overline{(\{4\})} = (\{A, B, C\}) \wedge \{1, 2, 3\}$. We can interpret this reject box as: T will reject any observation with $x_1 \in \{A, B, C\}$ and $x_2 \in \{1, 2, 3\}$; otherwise, T will certify it.

As another important remark, beyond the observations in E used to learn T , T will also certify the unseen observations $(D, 2)$, $(D, 3)$ and $(D, 4)$. This is an example of the *generalization* provided by encoding constraints of cardinality $k = 1$.

$k = 2$. We now continue with learning a constraint theory with cardinality $k = 2$. Again, consider the space of possible constraints whose literals have cardinalities $k = 2$:

$$\begin{aligned}
& (\{A, B\} \vee \{1, 2\}) \wedge (\{A, B\} \vee \{1, 3\}) \wedge (\{A, B\} \vee \{1, 4\}) \wedge \\
& (\{A, B\} \vee \{2, 3\}) \wedge (\{A, B\} \vee \{2, 4\}) \wedge (\{A, B\} \vee \{3, 4\}) \wedge \\
& (\{A, C\} \vee \{1, 2\}) \wedge (\{A, C\} \vee \{1, 3\}) \wedge (\{A, C\} \vee \{1, 4\}) \wedge \\
& (\{A, C\} \vee \{2, 3\}) \wedge (\{A, C\} \vee \{2, 4\}) \wedge (\{A, C\} \vee \{3, 4\}) \wedge \\
& (\{A, D\} \vee \{1, 2\}) \wedge (\{A, D\} \vee \{1, 3\}) \wedge (\{A, D\} \vee \{1, 4\}) \wedge \\
& (\{A, D\} \vee \{2, 3\}) \wedge (\{A, D\} \vee \{2, 4\}) \wedge (\{A, D\} \vee \{3, 4\}) \wedge \\
& (\{B, C\} \vee \{1, 2\}) \wedge (\{B, C\} \vee \{1, 3\}) \wedge (\{B, C\} \vee \{1, 4\}) \wedge \\
& (\{B, C\} \vee \{2, 3\}) \wedge (\{B, C\} \vee \{2, 4\}) \wedge (\{B, C\} \vee \{3, 4\}) \wedge \\
& (\{B, D\} \vee \{1, 2\}) \wedge (\{B, D\} \vee \{1, 3\}) \wedge (\{B, D\} \vee \{1, 4\}) \wedge \\
& (\{B, D\} \vee \{2, 3\}) \wedge (\{B, D\} \vee \{2, 4\}) \wedge (\{B, D\} \vee \{3, 4\}) \wedge \\
& (\{C, D\} \vee \{1, 2\}) \wedge (\{C, D\} \vee \{1, 3\}) \wedge (\{C, D\} \vee \{1, 4\}) \wedge \\
& (\{C, D\} \vee \{2, 3\}) \wedge (\{C, D\} \vee \{2, 4\}) \wedge (\{C, D\} \vee \{3, 4\})
\end{aligned}$$

After applying Valiant's algorithm to this batch of clauses with E , the learned constraint theory is then:

$$\begin{aligned}
T = & (\{A, B\} \vee \{1, 4\}) \wedge (\{A, C\} \vee \{1, 4\}) \wedge (\{A, D\} \vee \{1, 4\}) \wedge \\
& (\{A, D\} \vee \{2, 4\}) \wedge (\{A, D\} \vee \{3, 4\}) \wedge (\{B, C\} \vee \{1, 4\}) \wedge \\
& (\{B, D\} \vee \{1, 4\}) \wedge (\{B, D\} \vee \{2, 4\}) \wedge (\{B, D\} \vee \{3, 4\}) \wedge \\
& (\{C, D\} \vee \{1, 4\}) \wedge (\{C, D\} \vee \{2, 4\}) \wedge (\{C, D\} \vee \{3, 4\})
\end{aligned}$$

Here, we observe that the union of the reject boxes produced by clauses that contain D is *exactly identical to the reject box produced by clause* $(\{D\} \vee \{4\})$. Any observation will only satisfy those clauses in T if the observation has $x_1 = D$ or $x_2 = 4$. However, we do note that there are some unique clauses that produce reject boxes that are not a direct subset of the reject box produced by clause $(\{D\} \vee \{4\})$. Namely, $(\{A, B\} \vee \{1, 4\})$, $(\{A, C\} \vee \{1, 4\})$, and $(\{B, C\} \vee \{1, 4\})$. Of these unique clauses, without loss of generality, consider the reject box produced by $(\{A, B\} \vee \{1, 4\})$, that is: $(\{C, D\} \wedge \{2, 3\})$.

Now, we draw a reject box for this clause in orange and the union of the reject boxes for clauses containing D in red, shown in Figure 8. In this setting, we can see that the learned constraint theory is *less general*: T certifies five observations and rejects eleven (i.e., $|\psi_2| = 11$). Thus far, we have shown $|\psi_1| < |\psi_2|$.

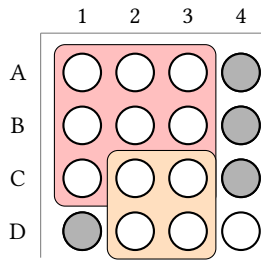


Figure 8: Reject space for $k = 2$ —In addition to the observations rejected for $k = 1$ (shown in red), observations $(D, 2)$ and $(D, 3)$ are also rejected when $k = 2$ (shown in orange).

From this, we make two important observations: (1) the size of the reject boxes are inversely proportional to the cardinality of the literals (i.e., the constraints are becoming *more granular* and *less general*), and (2) in addition to the observations rejected when

$k = 1$, observations $(D, 2)$ and $(D, 3)$ are now also rejected by T . In the context of generalization, beyond the observations used to learn T , only the unseen observation $(D, 4)$ will be certified by T when $k = 2$.

$k = n - 1 = 3$. We now finish with learning a constraint theory with cardinality $k = 3$ (note that, for this domain, $n = 4$, and thus, any clause with literals of cardinality four will be axiomatically satisfied, and so the maximum cardinality we consider is $n - 1 = 3$). We compute the last batch of the space of possible of constraints for $k = 3$:

$$\begin{aligned}
& (\{A, B, C\} \vee \{1, 2, 3\}) \wedge (\{A, B, C\} \vee \{1, 2, 4\}) \wedge (\{A, B, C\} \vee \{1, 3, 4\}) \wedge \\
& (\{A, B, C\} \vee \{2, 3, 4\}) \wedge (\{A, B, D\} \vee \{1, 2, 3\}) \wedge (\{A, B, D\} \vee \{1, 2, 4\}) \wedge \\
& (\{A, B, D\} \vee \{1, 3, 4\}) \wedge (\{A, B, D\} \vee \{2, 3, 4\}) \wedge (\{A, C, D\} \vee \{1, 2, 3\}) \wedge \\
& (\{A, C, D\} \vee \{1, 2, 4\}) \wedge (\{A, C, D\} \vee \{1, 3, 4\}) \wedge (\{A, C, D\} \vee \{2, 3, 4\}) \wedge \\
& (\{B, C, D\} \vee \{1, 2, 3\}) \wedge (\{B, C, D\} \vee \{1, 2, 4\}) \wedge (\{B, C, D\} \vee \{1, 3, 4\}) \wedge \\
& (\{B, C, D\} \vee \{2, 3, 4\})
\end{aligned}$$

Here, it is worth noting an important observation: *each of these clauses will fail to be satisfied by one and only one observation* (i.e., the size of the reject boxes for each clause at $k = 3$ is one-by-one). After applying Valiant's algorithm with E , the following constraint theory is learned:

$$\begin{aligned}
T = & (\{A, B, C\} \vee \{1, 2, 3\}) \wedge (\{A, B, C\} \vee \{1, 2, 4\}) \wedge \\
& (\{A, B, C\} \vee \{1, 3, 4\}) \wedge (\{A, B, D\} \vee \{1, 2, 4\}) \wedge \\
& (\{A, B, D\} \vee \{1, 3, 4\}) \wedge (\{A, B, D\} \vee \{2, 3, 4\}) \wedge \\
& (\{A, C, D\} \vee \{1, 2, 4\}) \wedge (\{A, C, D\} \vee \{1, 3, 4\}) \wedge \\
& (\{A, C, D\} \vee \{2, 3, 4\}) \wedge (\{B, C, D\} \vee \{1, 2, 4\}) \wedge \\
& (\{B, C, D\} \vee \{1, 3, 4\}) \wedge (\{B, C, D\} \vee \{2, 3, 4\})
\end{aligned}$$

Our observation that the reject boxes for $k = 3$ is one-by-one is further evidence by the fact that *the learned constrained theory T is missing exactly four clauses, one clause for each observation in E* .

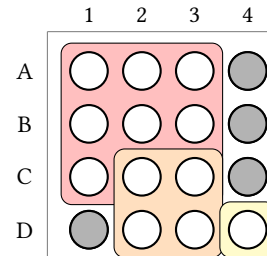


Figure 9: Reject space for $k = 3$ —In addition to the observations rejected for $k = 1$ (shown in red) and $k = 2$ (shown in orange), observations $(D, 4)$ is also rejected when $k = 3$ (shown in yellow).

In this setting, only one clause produces a reject box for a new observation beyond the reject boxes produced by clauses at $k = 2$: $(\{A, B, C\} \vee \{1, 2, 3\})$, with inverse $(\{D\} \wedge \{4\})$, as shown in yellow in Figure 9. In this setting, $k = n - 1$ results in a learned theory that

“overfits” to the training set E : T certifies only observations from E and rejects all other observations. Thus, T is *rigid*, i.e., it is *least general*. Finally, we observe that T certifies four samples and rejects twelve, i.e., $|\psi_3| = 12$.

Given a domain X , which contains X_i , the set containing all possible values for feature i , and a set of observations ψ_k that are rejected by a constraint theory T_k , which is a conjunction of clauses t , where t is a disjunction of literals $l_{k,i}$, which contain k values of feature i , we provide a general proof that $\psi_k \subseteq \psi_{k+1}$ (i.e., $\forall e, e \in \psi_k \implies e \in \psi_{k+1}$).

PROOF. Consider any $e \in \psi_k$, $1 \leq k < n - 1$, $n \geq 3$. Without loss of generality we assume that every feature space X_i is of size n . There must be some clause $t \in T_k$ that e does not satisfy of the form:

$$t = \bigvee_i l_{k,i}$$

With

$$l_{k,i} \subset X_i \wedge |l_{k,i}| = k \wedge e_i \notin l_{k,i}$$

Where t describes the disjunction of literals $l_{k,i}$ of size k that, for every feature i , contain a set of values that are within X_i , but do

not contain the value e_i . Now, we can build t' , which is the clause t with an additional value, $v_{k,i}$, in each literal:

$$t' = \bigvee_i l_{k,i} \cup \{v_{k,i}\}$$

With

$$v_{k,i} \notin l_{k,i} \wedge v_{k,i} \subset X_i \wedge e_i \neq v_{k,i}$$

Where t' is now clause t with an additional value $v_{k,i}$ in each literal, where $v_{k,i}$ is within the set of all values for the feature i , but is not equal to e_i .

Now, by construction, we have $t' \in T_{k+1}$, because literals are of size $k + 1$ and the clause is strictly less constrained than t , since the literals of t' can be satisfied by more samples than the literals of t . Since $t' \in T_{k+1}$, and we know that t' rejects e because $\forall i, e_i \notin l_{k,i}$ (i.e., t rejects e) and $\forall i, e_i \neq v_{k,i}$, which gives us $\forall i, e_i \notin l_{k+1,i}$ where $l_{k+1,i} = l_{k,i} \cup \{v_{k,i}\}$. Therefore, we have that $e \in \psi_{k+1}$. By induction, it can then be shown that:

$$\psi_1 \subseteq \dots \subseteq \psi_k \subseteq \psi_{k+1} \subseteq \dots \subseteq \psi_{n-1}$$

□

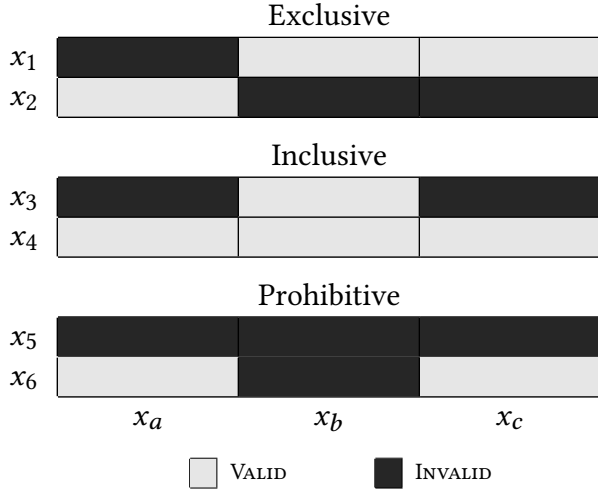


Figure 10: Constraint Types – An example visualization of three kinds of learned constraints between network protocols (e.g., x_1, x_2, \dots, x_6) and services (e.g., x_a, x_b , & x_c)

B RATIONALIZING DOMAIN CONSTRAINTS

Here, we provide supplementary material on a conceptual model characterizing the learned constraints by Valiant’s algorithm into one of three types, as shown in Figure 10. Valiant’s algorithm learns these three types of constraints simultaneously; we found this conceptual model helping in rationalizing the learned constraints.

Exclusive Constraints. Exclusive constraints are perhaps the most intuitive types of relationships; they describe one-to-one mappings between two variables. A constraint \mathcal{C} between X_α and X_β is said to be *exclusive*, if:

$$\exists x_a \in X_\beta, \forall (x_1, x_2) \in X_\alpha^2, \mathcal{C}(x_1, x_a) \wedge \mathcal{C}(x_2, x_a) \implies x_1 = x_2$$

where $\mathcal{C}(x, y)$ is an indicator function that a constraint exists between two variables x and y . Thematically similar to definitions for injective functions, exclusive constraints encode that if a constraint exists between variables x_a and x_1 , then x_a does not have a constraint for any other variable in the domain for which x_1 belongs to. Conceptually, we can imagine such constraints between network

services and protocols. As an example, we can expect that some services, such as SSH, can only be used with TCP.

Inclusive Constraints. Unlike exclusive, inclusive constraints describe one-to-many mappings. Again, a constraint \mathcal{C} between X_α and X_β is said to be *inclusive*, if:

$$\exists x_a \in X_\beta, \forall (x_1, x_2) \in X_\alpha^2, \mathcal{C}(x_1, x_a) \wedge \mathcal{C}(x_2, x_a) \not\Rightarrow x_1 = x_2$$

In other words, it is *not* necessary for x_1 and x_2 to be the same variable if there exists constraints $\mathcal{C}(x_1, x_a)$ and $\mathcal{C}(x_2, x_a)$. We can again imagine a scenario where a service, for example NTP, can be used with multiple protocols, such as TCP and UDP.

Prohibitive Constraints. We call the final constraint type prohibitive constraints. These constraints describe regions for which no observation can exist⁵. We formalize a prohibitive constraint \mathcal{C} between X_α and X_β as:

⁵There are constraint learning approaches that leverage *negative examples*, which are realizations of inputs that cannot exist. Practical datasets used for machine learning $\forall x_1 \in X_\alpha, \nexists x_a \in X_\beta$ such that $\mathcal{C}(x_1, x_a) = 1$

Prohibitive constraints are especially interesting. At first, they seem redundant (one could consider invalid regions to simply be the dual of valid regions) or non-informative (a variable in a dataset that has no observation surely cannot be useful to any learning algorithm). The necessity of prohibitive constraints is rooted in learning relationships with variables that live in a *continuous* domain. While such variables can take any real value in theory, there exists real-world phenomena for which continuous variables instead take values that can be approximated as discrete clusters of values. Prohibitive constraints grant us the flexibility to learn such phenomena.

As an example from networks, consider packet sizes; it is a well-known phenomena that packet sizes on the Internet closely follow a bimodal distribution [64, 70] (i.e., packet lengths are either small or large). Consider this observation at the extreme, that is, let the two modes be non-overlapping. In a practical setting, this means that the *largest* packet from the “small” distribution is smaller than the *smallest* packet from the “large” distribution. Variables that describe continuous phenomena can exhibit these regions and prohibitive constraints are necessary to model these contexts.

do not provide such examples, and thus prohibitive constraints give us the flexibility to *infer* negative examples from gaps between values in positive examples.

Symbol	Meaning
Universal	
e	sample or observation
E	dataset or collection of observations
Machine Learning	
e^*	adversarial example
y	sample label
θ	model parameters
f_θ	model with parameters θ
J	Jacobian of a model
S	Saliency Map
\hat{y}	model prediction
α	perturbation magnitude
p	parameter for some ℓ_p -norm
ϕ	budget (measured as a distance)
\mathcal{B}_ϕ	norm-ball of radius ϕ
Formal Logic	
\vdash	logical entailment
\in	set membership
X	domain
X_i	i th feature (or variable) space
x_i	some value for feature i
C	possible constraints from a domain
t	a clause in a constraint theory
T	a constraint theory
H	a constraint theory with partial assignments
ψ	set of observations rejected by a constraint theory
P	Pseudo-power set
p	set within some pseudo-power set
Ξ	space of possible observations
Λ	constraint-compliant set of observations
Ψ	constraint-noncompliant set of observations

Table 6: Symbols used in this paper

C MISCELLANY

Dataset	Features
NSL-KDD	1.Flag
	2.Src Bytes
	3.Dst Bytes
	4.Land
	5.Num Compromised
	6.Srv Serror Rate
	7.Rerror Rate
	8.Diff Srv Rate
	9.Srv Diff Host Rate
	10.Dst Host Srv Serror Rate
	11.Dst Host Rerror Rate
Phishing	1.UrlLength
	2.NumNumericChars
	3.NumSensitiveWords
	4.PctExtHyperlinks
	5.PctNullSelfRedirectHyperlinks
	6.FrequentDomainNameMismatch
	7.SubmitInfoToEmail
	8.PctExtResourceUrlsRT
	9.ExtMetaScriptLinkRT
	10.PctExtNullSelfRedirectHyperlinksRT

Table 4: Features

C.1 Hyperparameters

Dataset	# Neurons per Hidden Layer	Learning Rate	Iterations
NSL-KDD	60, 32	10^{-3}	16
Phishing	20	10^{-2}	15

Table 5: Hyperparameters

For our models, we use multilayer-perceptrons using ADAM optimizer. Hyperparameters are shown in Table 5.

C.2 Table of Symbols

C.3 Dataset Details

Table 4 shows the features used in our datasets after feature reduction. Details on the meaning behind the features can be found in [63] for the NSL-KDD and in [16] for Phishing.

C.4 DPLL

Constraint learning is a historical problem in computer science and shares many parallels with satisfiability problems. While constraint learning tries to learn what the constraints are, satisfiability attempts, as the name suggests, to return an assignment that satisfies a set of boolean expressions.

For constraint satisfaction, we use DAVIS-PUTNAM-LOGEMAN-LOVELAND (DPLL) [17], shown in Algorithm 3. DPLL has some characteristics that make it ideal for our task, namely: (1) it accepts boolean formulae in CNF, which is the native form of the constraint theories learned by Valiant’s Algorithm, and (2) it is a *backtracking-based* search algorithm. DPLL iteratively builds candidate solutions for a given expression, which is a property we exploit, detailed in Section 4.5.

DPLL frames constraint satisfaction as a search problem; first initialized with a set of boolean clauses H containing unassigned literals, the algorithm first assigns a literal l to either TRUE or FALSE, and recursively calls itself with the new assignment for l . DPLL returns FALSE if a contradiction is reached or TRUE if all literals are assigned. DPLL has a runtime advantage over other backtracking algorithms as it performs two simplifications to H at each call: `UnitPropagate` and `PureLiteralElimination`. `UnitPropagate` assigns values to literals who are the only members of their clauses (as only one assignment makes such clauses true). `PureLiteralElimination` assigns the necessary value to literals who are *pure*, that is, a literal l is either l or $\neg l$ for all clauses in H . Therefore, such literals can be assigned so that all clauses containing them are true.

Input: set of boolean clauses H
Output: a truth value

```

1 if  $H$  contains a contradiction then
2   | return FALSE
3 end
4 if  $H$  contains an assignment for every variable then
5   | return TRUE
6 end
7 for  $C^* \in \{C \mid C \in H \wedge |C| = 1\}$  do
8   |  $H \leftarrow \text{UnitPropagate}(C, H)$ 
9 end
10 for  $l^* \in \{l \mid l \in H \wedge \text{Pure}(l)\}$  do
11   |  $H \leftarrow \text{PureLiteralElimination}(l^*, H)$ 
12 end
13  $l \leftarrow$  arbitrarily select an unassigned literal
14 if  $\text{DPLL}(H \cup \{l \leftarrow \text{TRUE}\}) = \text{TRUE}$  then
15   | return TRUE
16 end
17 else
18   | return  $\text{DPLL}(H \cup \{l \leftarrow \text{FALSE}\})$ 
19 end

```

Algorithm 3: Davis-Putnam-Logemann-Loveland

C.5 Constraint Representation

Recall Valiant’s algorithm; it determines if an observation e complies with a constraint theory T by iterating over all clauses $t \in T$ and evaluating if at least one literal in t is satisfied by the feature values of e . Depending on the cardinality of each literal, determining if a clause is satisfied through a linear search could be intractable. Instead, we use a set-based representation for literals as this reduces clause satisfaction to be on the order of the number of literals in the clause (since set-membership queries can be done in constant time).

While this optimization is appropriate for boolean and categorical features, continuous features require a different representation to be efficient. Recall that we leverage OPTICS to cluster feature values into discrete bins representing sets of ranges (e.g., $\{x \mid (0.25 \leq x < 0.50) \vee (0.75 \leq x < 1.00)\}$). Thus, checking if clauses are satisfied with continuous features can be done in $\mathcal{O}(\log(n))$ time with binary search, where n describes the number of bins.

In practice these optimizations yielded a tractable constraint learning process. The NSL-KDD constraint generation process executed in just over 3 days, and the phishing dataset completed in about 1 day (with OPTICS consuming the vast majority of time, detailed in Section 5.5). Note that learning need only be executed once for a set of training data. Moreover, there are algorithmic optimizations that could enable the integration of new data in an incremental way [44]. We will explore these techniques in future work.